Jorge Filipe Mónico Delgado

Buracos Negros de Kerr com Carga Elétrica e Cabelo Escalar

Kerr Black Holes with Electric Charge and Scalar Hair

Jorge Filipe Mónico Delgado

Buracos Negros de Kerr com Carga Elétrica e Cabelo Escalar

Kerr Black Holes with Electric Charge and Scalar Hair

"I want to know God's thoughts; the rest are details."

— Albert Einstein

Jorge Filipe Mónico Delgado

Buracos Negros de Kerr com Carga Elétrica e Cabelo Escalar

Kerr Black Holes with Electric Charge and Scalar Hair

Dissertação apresentada à Universidade de Aveiro para cumprimento dos requisitos necessários à obtenção do grau de Mestre em Mestrado em Física, realizada sob a orientação científica do Prof. Dr. Carlos Alberto Ruivo Herdeiro, Investigador Principal do Departamento de Física da Universidade de Aveiro, e Dr. Eugen Radu, Investigador Principal do Departamento de Física da Universidade de Aveiro.

O Júri / The jury

Presidente / President

Prof. Dr. Manuel António dos Santos Barroso
Professor Auxiliar do Departamento de Física da Universidade de Aveiro

Vogais / Committee

Prof. Dr. Carlos Alberto Ruivo Herdeiro
Investigador Principal do Departamento de Física da Universidade de Aveiro (orientador)

Prof. Dr. Filipe Artur Pacheco Neves Carteado Mena
Professor Associado do Departamento de Matemática e Aplicações da Universidade do Minho (examinador)

Agradecimentos / Acknowledgements

First and foremost I offer my greatest gratitude to my supervisor, Prof. Dr. Carlos Alberto Ruivo Herdeiro and to my co-supervisor, Dr. Eugen Radu, whose support was undoubtedly the best one can have. This thesis was only possible due to all the patience of both to answering all of my questions and to all of the encouragement and effort of both. I also offer my gratitude to my colleague Helgi Freyr Rúnarsson for all the help, patience and support. I hope to continue to work with all of them in the future.

To Professor Manuel Barroso and Ricardo Dias for their support and guidance throughout the entire degree.

I would like to thank my roommate Miguel Ferreira and former roommate David Pereira for the best years of my academic life. Without them I would not have nearly a quarter of the good memories and stories that I have. I am really glad and thankful to have had the privilege to have lived with them.

To my dearly beloved Ana Pedro Paracana, I would like to give my biggest thank for everything I am now. If I could I would list everything that she taught me and showed me, but, sincerely, this page is not long enough. The more confident and less anxious person that I am now, was born because of her, and for that, there is not a big enough thank that can express my gratitude for everything that she did for me. I also would like to give my thank to her sister, Ana Rita Paracana, for the company and the conversations, proving me that one does not need to know physics to be curious about it.

I want to thank Diamantino Silva, Ivo Maceira and Raul Costa for all their help, their encouragement and, above all, for the patience to put up with me, I know that was not easy. I also want to thank particularly my "sister" Sílvia Reis for being there whenever I needed and for being one of the best friendships I made in my academic years. To João Peixoto and André Ferreira, for being the coolest freshmen I ever met and for all the fun we had, and will have. To "11 da vida airada" for all the good memories we share together, and for all the new ones that are to come. In particular, I want to give a special thank to a person of this group, Carolina Gouveia, for all her help and wisdom so I could overcome some obstacles. To all the my fellow colleagues from the Physics Department, namely from FISUA, for all the help that everyone gave me.

Last but definitely not least, I want to express my gratitude to my family for supporting me at all times, for giving me the opportunity to pursue my dreams and for everything that they taught me. I am where I am and I had, and have, everything because of my family, and for that I can not thank them enough. I am really thankful for having them all by my side.

Resumo

A solução de Kerr [Kerr, 1963] descreve um buraco negro (BN) em rotação no vácuo em Relatividade Geral (RG). Pouco depois da sua descoberta, uma generalização electricamente carregada deste BN foi encontrada [Newman et al., 1965]. No início dos anos 70, poderosos teoremas de unicidade foram estabelecidos em RG, para o vácuo e electro-vácuo, demonstrando que estas são as soluções de BN mais gerais, fisicamente aceitávies, no vácuo ou electro-vácuo. Estas descobertas levaram a duas ideias, amplamente difundidas, mas não demonstradas: 1) BNs não têm "cabelo" [Ruffini and Wheeler, 1971], $i.e$, mesmo na presença de conteúdos de matéria mais genérica, soluções de BNs devem ser descritas simplesmente pela sua massa, momento angular e outras cargas associadas a uma lei de Gauss; 2) alguns limites específicos na carga e no momento angular observados para estas soluções são genéricos para BNs.

Contudo, recentemente foi descoberto que BNs conseguem ter "cabelo" escalar [Herdeiro and Radu, 2014]. Estas soluções, designadas *BNs de Kerr com cabelo escalar* (BNsKCE), revelaram um mecanismo que permite BNs de Kerr ter cabelo de diferentes campos (escalar, vectorial,...) e com diferentes propriedades.

Nesta tese, depois de uma breve revisão sobre soluções padrão de BNs em RG, começaremos por revisitar algumas das técnicas que permitem a construção de BNsKCE, que obtivemos numericamente. Iremos ilustrar o procedimento construindo a conhecida solução de Kerr numericamente, que nos permite testar a exatidão do método. Iremos seguidamente introduzir algumas quantidades físicas de interesse para BNs, relevantes para os limites acima mencionados e ilustrar os seus cálculos num BN de Kerr-Newman e Kerr-Sen. Isto permitir-nos-á estabelecer que estes limites são violados em termos das quantidades calculadas no *horizonte* para estas soluções. Isto também é o caso dos BNsKCE, no qual, contudo, estes limites podem ser violados, mesmo em termos de quantidades assimptóticas. Finalmente iremos contruir BNsKCE electricamente carregados e estudar algumas das suas propriedades físicas. Em particular, mostraremos que o factor giromagnético, g, destas soluções obedece a $g \leqslant 2$.

Abstract

The Kerr solution [Kerr, 1963] describes a rotating black hole (BH) in vacuum General Relativity (GR). Shortly after its discovery, an electrically charged generalization thereof was found [Newman et al., 1965]. In the 1970s, powerful uniqueness theorems were established in vacuum and electro-vacuum GR, demonstrating these are the most general, physically acceptable, single BH solutions in vacuum or electro-vacuum GR. These findings led to two widespread beliefs: 1) BHs have "no-hair" [Ruffini and Wheeler, 1971], $i.e$, even in the presence of more generic matter contents, BH solutions should be described by only their mass, angular momentum and other charges associated to Gauss laws; 2) some particular bounds on the charge and angular momentum observed for these solutions are generic for BHs.

Recently, however, it was found that BHs can carry scalar "hair" [Herdeiro and Radu, 2014]. These solutions, called *Kerr BHs with scalar hair* (KBHsSH), unveiled a mechanism that allows Kerr BHs to carry hair of different fields (scalar, vector,...) and with different properties.

In this thesis, after a brief review of the standard BH solutions in GR, we will start by revisiting some of the techniques that allowed the construction of KBHsSH, that were obtained numerically. We shall illustrate the procedure by constructing the well known Kerr solution numerically, which allows us to test the accuracy of the method. We will then introduce some physical quantities of interest for BHs, relevant for the aforementioned bounds and illustrate their computation in Kerr-Newman and Kerr-Sen BHs. This will allow us to establish that these bounds are violated in terms of *horizon* quantities for these solutions. This is also the case for KBHsSH, for which, however, these bounds can be violated even in terms of asymptotic quantities. Finally we will construct electrically charged KBHsSH and study some of their physical properties. In particular we will show that the gyromagnetic ratio, g, of these solutions obeys $g \leqslant 2$.

Contents

List of Figures

Chapter 1

Introduction

On September 14th 2015, the advanced Laser Interferometer Gravitational-Wave Observatory (aLIGO) registered a gravitational wave (GW) signal (GW150914), opening the era of GW astronomy [1]. This new window to the Cosmos will unveil the Gravitational Universe, probing the strong and dynamical field regime of gravity and testing the limits of Einstein's theory and its paradigmatic predictions [2].

Amongst the theoretical predictions of General Relativity (GR), a most remarkable one, anchored on the celebrated uniqueness theorems [3], is that the end point of gravitational collapse is a Kerr black hole (BH) [4], and hence fully characterized by two parameters, mass and angular momentum. Such simplicity of BHs in vacuum GR (but generalizable to electro-vacuum), gave rise to the belief that it holds also in the presence of generic physical matter. This is the no-hair hypothesis [5]. If true, it signifies that BHs are extraordinarily simple and special objects, and it lies at the centre of many current discussions of astrophysical BH candidates. Testing this hypothesis, using the latest theoretical, technical and observational developments is a central goal of the strong gravity community for the coming years.

On the theoretical side, the last two years saw interesting developments. New families of BHs with scalar hair [6, 7] have been found - *Kerr BHs with scalar hair* (KBHsSH). These solutions are continuously connected to Kerr BHs, and yield qualitatively new examples of hairy BHs, with potential astrophysical relevance as they connect between the paradigmatic BH solution (the Kerr one) and dark matter candidates known as boson stars [8]. Even more importantly, the discovery of these solutions uncovered a new and quite generic mechanism [9], that can be used to construct many solutions of hairy BHs, both in the presence of more general scalar fields, *e.g.* with self interactions [10], and for other fields, such as spin 1 [11] and 2 massive fields.

The purpose of this thesis is two-fold. On the one hand, we wish to understand better some physical properties of these new hairy solutions. Specifically, it was observed that these solutions can violate the Kerr bound both in terms of asymptotic [6, 7] and horizon quantities [9]. In particular, the latter, were found surprising by a part of the community. Here, we shall point out that something similar occurs for other, well known solutions of General Relativity coupled to gauge fields, namely the Kerr-Newman [12] and the Kerr-Sen [13] solutions, which are known in closed form. These findings were reported in a recently published work [14], co-authored by the author of this thesis. On the other hand, we shall construct electrically charged generalizations of KBHsSH, by considering Einstein-Maxwell-Klein-Gordon theory, where the scalar field may or may not be gauged. These solutions are

constructed using the same numerical techniques that allowed the construction of KBHsSH. We shall then explore some physical properties of these charged hairy BHs. In particular we will discuss that the gyromagnetic ratio decreases when scalar hair exists, as compared to that of the Kerr-Newman BH, which takes the (non-anomalous) electron value $g = 2$ [15]. This study was reported in (another) recently published paper, also co-authored by the author of this thesis [16].

This thesis is organized as follows: in Chapter 2, a brief review of well known solutions of the Einstein equations is presented. Since we are interest in numerical solutions, a review of the numerical solver we used, together with an example, will be given in Chapter 3. After that, we will focus on one of the main topic of this thesis, which is the physical quantities of a BH, starting by describing the theory behind the computation of such quantities, and then applying the theoretical result to two known solutions: the Kerr-Newman and the Kerr-Sen solutions. This study can be found in Chapter 4 and includes some original results published in [14]. Next, we move on to the second main topic of this thesis: Hairy BHs. This topic is quite vast, so we have decided to divide it into two chapters. The first one, Chapter 5, gives the reader a reason why BHs with (physically reasonable) scalar hair were considered impossible to exist for so many years, in contrast with other types of hairy BHs. However, this chapter gives also hope, because we provide a way to work around the previous reason. Building upon this hope, we describe the existence of Kerr BHs with scalar hair, where we go through the setup we used to reconstruct them, the results we have obtained, and also some of their physical properties. In the second chapter of this second main topic, Chapter 6, we present our latest original work, published in [16], where we have obtain numerically the electric generalization of Kerr BHs with scalar hair. In this chapter we consider two different cases: one where only the BH is electrically charged; and another where both the BH and the scalar hair are electrically charged. In both cases we follow a similar strategy as we used in the previous chapter, presenting the setup, the results and some physical properties. Finally, in Chapter 7, we give some final remarks and conclusions about this thesis.

Chapter 2

Topics of BH Physics

One of the most remarkable predictions of GR is the existence of super compact objects that greatly deform the spacetime surrounding them, dubbed BHs. Such objects were vastly studied in the last century and still are greatly studied in the present one, with the goal of understanding strong gravity. In particular, many BH solutions have been found for the Einstein equations, with different types of matter.

The first, and simpler, BH solution ever discovered was found by Karl Schwarzschild precisely one century ago, in 1916. Schwarzschild solved the vacuum Einstein equations,

$$R_{\mu\nu} - \frac{1}{2} g_{\mu\nu} R = 0 \,, \tag{2.1}$$

by assuming a spherically symmetric and static spacetime [17]. Thus, this solution describes a spherically symmetric, static and asymptotically flat BH, and its metric can be written[1], in Schwarzschild coordinates (t, r, θ, φ), as,

$$ds^2 = -\left(1 - \frac{2M}{r}\right) dt^2 + \left(1 - \frac{2M}{r}\right)^{-1} dr^2 + r^2 \left(d\theta^2 + \sin^2\theta d\varphi^2\right) \,, \tag{2.2}$$

where M is the mass of the BH. As expressed by the above line element, the corresponding BH, dubbed *Schwarzschild* BH, is only characterised by the total mass of the BH.

A few years after this discovery, a new family of solutions was found, generalizing spherically symmetric BHs to Einstein-Maxwell theory, *i.e.*, Einstein's gravity minimally coupled to source free Maxwell's electromagnetism. The action of such theory reads,

$$\mathcal{S} = \frac{1}{16\pi} \int d^4x \sqrt{-g} \left(R - F_{\mu\nu} F^{\mu\nu}\right) \,, \tag{2.3}$$

where $F_{\mu\nu}$ are the components of the Maxwell 2-form, F, related to the 1-form potential $A = A_\mu dx^\mu$ as $F = dA$, which yield the Einstein-Maxwell equations,

$$R_{\mu\nu} - \frac{1}{2} g_{\mu\nu} R = 2\left(F_\mu{}^\rho F_{\nu\rho} - \frac{1}{4} g_{\mu\nu} F_{\rho\sigma} F^{\rho\sigma}\right) \,, \qquad D_\nu F^\nu{}_\mu = 0 \,, \tag{2.4}$$

where D_ν is the covariant derivative. The first solution of such family was found by Hans Reissner in 1916 [18], and two years later completed by Gunnar Nordström [19]. This solution was obtain using basically the same assumptions that Schwarzschild used to obtain his

[1] It is important to note that, throughout this thesis, we are using the signature $(-,+,+,+)$ and natural units such that $G = 1$, $c = 1$ and $4\pi\epsilon_0 = 1$.

solution, but, in this case, we are in a electro-vacuum spacetime, thus the energy-momentum tensor is non-zero. Nevertheless, the *Reissner-Nordström* (RN) solution describes a spherical symmetric, static and asymptotically flat BH, and can be written, in Schwarzschild-type coordinates, as,

$$ds^2 = -\left(1 - \frac{2M}{r} + \frac{Q_E^2}{r^2}\right) dt^2 + \left(1 - \frac{2M}{r} + \frac{Q_E^2}{r^2}\right)^{-1} dr^2 + r^2 \left(d\theta^2 + \sin^2\theta d\varphi^2\right) , \quad (2.5)$$

$$A_\mu dx^\mu = -\frac{Q_E}{r} dt , \quad (2.6)$$

where Q_E is the electric charge of the BH. It is easy to see that this metric is an electric generalization of the Schwarzschild one and that a RN BH is characterised now by its total mass and electric charge.

A more general solution of the vacuum Einstein equations only appear almost 50 years later, in 1963, when Roy Kerr found a rotating solution that could solve such equations [4]. To achieve that, Kerr imposed an axially symmetric and stationary spacetime, instead of a spherically symmetric and static one. With these new assumptions, Kerr arrived to the following metric, here written in Boyer-Lindquist (BL) coordinates,

$$ds^2 = -\frac{\Delta}{\Sigma}\left(dt - a\sin^2\theta\right)^2 + \Sigma\left(\frac{dr^2}{\Delta} + d\theta^2\right) + \frac{\sin^2\theta}{\Sigma}\left[adt - \left(\Sigma + a^2\sin^2\theta\right)d\varphi\right]^2 \quad (2.7)$$

with $\Delta = r^2 - 2Mr + a^2$ and $\Sigma = r^2 + a^2\cos^2\theta$, where $a = J/M$ is the angular momentum per unit mass. Such metric yield a *Kerr* BH that is completely described by its total mass M and angular momentum J and, although it is not obvious, it is the rotating generalization of the Schwarzschild solution, which can be easily proven by taking the limit $a \to 0$.

Erza Newman and collaborators, in 1965, following a rather similar strategy to that Nordström used to obtain his solution, discovered a rotating solution that solved the electro-vacuum Einstein equations [12]. In this way, the solution Newman found is also an axisymmetric, stationary and asymptotically flat BH, dubbed *Kerr-Newman* (KN) BH, and its metric reads, in BL coordinates,

$$ds^2 = -\frac{\Delta}{\Sigma}\left(dt - a\sin^2\theta\right)^2 + \Sigma\left(\frac{dr^2}{\Delta} + d\theta^2\right) + \frac{\sin^2\theta}{\Sigma}\left[adt - \left(\Sigma + a^2\sin^2\theta\right)d\varphi\right]^2 , \quad (2.8)$$

$$A_\mu dx^\mu = -\frac{Q_E\, r}{\Sigma}\left(dt - a\sin^2\theta d\varphi\right) , \quad (2.9)$$

where, now, $\Delta = r^2 - 2Mr + a^2 + Q_E^2$ and $\Sigma = r^2 + a^2\cos^2\theta$. This BH is completely described by its total mass, angular momentum and electric charge and it is a generalization of the three previous BHs. Indeed: if one takes the limit $a \to 0$, one finds the RN solution; if one takes the limit $Q_E \to 0$, one obtains the Kerr solution; and if one takes both limits, one recovers the static vacuum Schwarzschild solution.

Other solutions were found throughout the years, using different matter contents and symmetries in GR and alternative models of gravity, but these four solutions are the most important ones because of how they changed our perspective about BH physics, and how simple and elegant they are. And since the core of this thesis is based in the Kerr and KN solution, we will not give further details about other solutions.

Chapter 3

Numerical Techniques: the FIDISOL/CADSOL Solver

The Einstein equations are, in general, a set of coupled nonlinear second order partial differential equations (PDEs), which makes extremely hard the quest of finding analytic solutions (*i.e* in closed form) such as the ones presented in the previous chapter. Then known cases have either a vanishing or a fairly simple energy-momentum tensor, and possess several symmetries. But for more complex cases it becomes increasingly difficult to obtain analytic solutions. As such, one may take the pragmatic approach of seeking numerical solutions, when the analytic approach fails.

There is a variety of numerical techniques one could use to tackle the Einstein equations, each of which could be more suitable for a specific class of problems. In our case, we shall be seeking for stationary solutions, and hence we need a numerical approach that can solve a set of coupled *elliptic* PDEs, rather than hyperbolic-like PDEs, as in a time evolution problem. Such numerical approach is provided by the professional package FIDISOL/CADSOL [20, 21, 22] written in F90. This software solves nonlinear systems of two-dimensional (and also three-dimensional) elliptic and parabolic partial differential equations, subject to arbitrary boundary conditions on a rectangular domain (or on any domain that can be analytically transform to a rectangular domain). FIDISOL/CADSOL uses a finite differences method, namely the Newton-Raphson method, with self-adaptative grid and consistency order, and can also provide error estimates for the computed solution, allowing the user to judge on its quality, as described in what follows.

The fact that this solver uses a Newton-Raphson method implies that it finds the roots of the equation(s). For the type of problems solved in this thesis, the differential equation(s) are written in the generic form

$$P(x, y; u; u_x, u_y; u_{xy}, u_{xx}, u_{yy}) = 0 \ , \tag{3.1}$$

where u is the set of function we want to compute and u_x, u_y and u_{xy}, u_{xx}, u_{yy} are the first, and, respectively, the second derivatives of the function(s) u with respect to the generic coordinates x and y (note that for the problems we solve, x, y are basically the spherical coordinates r, θ). Also, we have to compute the Jacobian for all the functions present in the equations, which is found by simple differentiation of each equation P with respect to $u; u_x, u_y; u_{xy}$ and u_{xx}, u_{yy}. One has also to supply an initial guess for each function u, together with the boundary conditions for u, and also a given mesh in x, y with $N_x \times N_y$ points. If

one already has all these requirements, one can implement the corresponding problem in the solver.

The numerical procedure works as follows [20, 21, 22] (note that the approach here is generic for the Newton-Raphson method): for an approximate initial solution $u^{(1)}$, $P(u^{(1)})$ does not vanish. In the next step one considers an improved solution

$$u^{(2)} = u^{(1)} + s\Delta u, \tag{3.2}$$

supposing that $P(u^{(1)} + s\Delta u) = 0$ (with s a relaxation factor, which is usually chosen as $s = 1$). The expansion in the small parameter Δu gives to first order

$$0 = P(u^{(1)} + \Delta u) \approx P(u^{(1)}) + \frac{\partial P}{\partial u}(u^{(1)})\Delta u \ + \dots \ . \tag{3.3}$$

This algebraic equation is used to determine the correction $\Delta u^{(1)} = \Delta u$. Then one repeats the calculation iteratively (*e.g.* $u^{(3)} = u^{(2)} + \Delta u$), such that the approximate solutions will converge (provided the initial guess was close enough to the true solution).

In each step, a linear system of algebraic equations is solved, and the residual $||P(u^{(i)})||$ decreases by a factor of approximately 10. As a generic feature of this approach, the iteration stops after N steps, when the Newton residual $P(u^{(N)})$ is smaller than a prescribed tolerance (which is an input parameter). Clearly, it is essential to have a good first guess, when starting the iteration procedure. Such dependence of the convergence on the initial guess is a disadvantage of this method (note that without a good enough initial guess, the solver will not converge to the true solution, giving us some random wrong answer). However, if we have a good understanding of the problem we plan to solve, we can find a reasonable initial guess for the functions, overcoming such a disadvantage.

The package FIDISOL/CADSOL provides also error estimates for each function, which provides us with a criteria to judge the quality of the computed solution. The errors are computed by the solver, on the "consistency level", namely, the discretized Newton residual, and as discretization error terms in x, y, z directions. The discretization error is estimated through the difference of difference quotients. For example, in Equation 3.3, the derivative of the solution u and of the correction function Δu are discretized by a difference method with arbitrary consistency orders. Also, the derivatives are replaced, for example, in the form $u_{xx} \Leftarrow u_{xx,d} + d_{xx}$, $\Delta u_{xx} \Leftarrow \Delta u_{xx,d}$ (where the index d means "*discretized*"). In this relation d_{xx} denotes the estimate for the discretization (or truncation) error of u_{xx}, defined as $d_{xx} = u_{xx,d,next} - u_{xx,d}$; the index "*next*" stays for the next higher member of the family of backward difference formulas. For convergent problems, the discretized Newton residual decreases with the number of Newton-Raphson iterations. Also, the discretization error terms depend on the grid size and the used consistency order, *i.e.* on the order of the discretisation of derivatives. Note that for the numerical results reported in this thesis, the order of the discretisation was typically six.

Apart from the error estimates provided by FIDISOL/CADSOL, we use other specific criteria to judge on the quality of the numerical results, as provided by the problem one solves (*e.g.* the Smarr law and/or the 1st law of thermodynamics when dealing with new classes of BH solutions). Examples of such tests are discussed in the next section.

Overall, this package is an excellent tool for the kind of problems we shall be interested, originating from the Einstein equations, yielding good quality solutions and corresponding error estimates within a reasonable amount of computational work. In the next section, we

illustrate this numerical approach by reconstructing, numerically, the Kerr solution. As the latter is known analytically, one can then compare the numerical and closed form solution, to gain insight on the overall quality of the method. Finally, let us remark that some of the new solutions derived by using the code FIDISOL/CADSOL were rederived subsequently by other groups with different numerical methods, see *e.g.* [23].

3.1 Examples: Kerr Solution

A good way to get a better intuition and understanding of the solver is by using it to reconstruct known solutions. Here we shall do so for the Kerr solution. In order to do that, one must define an ansatz for the metric and specify the boundary conditions to all the functions present in that ansatz. With this in mind, we take the following ansatz for the metric,

$$ds^2 = -e^{2F_0} N dt^2 + e^{2F_1} \left(\frac{dr^2}{N} + r^2 d\theta^2 \right) + e^{2F_2} r^2 \sin^2\theta (d\varphi - W dt)^2 \,, \tag{3.4}$$

where F_i, W, $i = 0, 1, 2$, are functions that only depend on r and θ, and $N \equiv 1 - r_H/r$, in which r_H is the event horizon radius. This form for the Kerr metric corresponds to a non-standard coordinate system that one does not find in a normal textbook. However, the coordinate transformation to the standard BL coordinates is quite simple, corresponding solely to a shift of the radial coordinate. Such transformation is provided in Appendix A.

Now that we have chosen the metric ansatz, we have to impose the boundary conditions for all the metric functions. Since the solutions we want to obtain are regular, stationary, axisymmetric and asymptotically flat, the boundary conditions will be imposed according to these requirements. In this way we impose the following boundary conditions [6, 7],

(i) *Asymptotic boundary conditions.* Asymptotically flatness implies that the solution must approach a Minkowski spacetime at spatial infinity, $r \to \infty$, thus,

$$\lim_{r\to\infty} F_i = \lim_{r\to\infty} W = 0 \,. \tag{3.5}$$

where $i = 0, 1, 2$.

(ii) *Axis boundary conditions.* At the poles, *i.e.* at $\theta = 0, \pi$, axial symmetry and regularity imply,

$$\partial_\theta F_i = \partial_\theta W = 0 \,. \tag{3.6}$$

Moreover, the absence of conical singularities implies also that $F_1 = F_2$ on the symmetry axis. Also, due to the symmetry with the equatorial plane we can further impose the following boundary condition on the equatorial plane,

$$\partial_\theta F_i|_{\theta=\pi/2} = \partial_\theta W|_{\theta=\pi/2} = 0 \,. \tag{3.7}$$

(iii) *Event horizon boundary conditions.* A coordinate transformation can be made in the form, $x = \sqrt{r^2 - r_H^2}$, to simplify the numerical treatment, and with such new coordinate

one can compute a power series expansion near the horizon, $x \to 0$, of the metric functions,

$$F_i = F_i^{(0)}(\theta) + x^2 F_i^{(2)}(\theta) + \mathcal{O}(x^4) \,, \tag{3.8}$$
$$W = \Omega_H + \mathcal{O}(x^2) \,. \tag{3.9}$$

With this result it is natural to impose the following boundary condition,

$$\partial_x F_i|_{r=r_H} = 0 \,, \qquad W|_{r=r_H} = \Omega_H \,. \tag{3.10}$$

The constant Ω_H can be immediately interpreted as the angular velocity of the horizon.

The next step is to impose the vacuum Einstein equations, Equation 2.1, to get the differential equations for the metric functions. Since the Einstein equations are non-linear and really tricky to compute by hand, we used the computational software MATHEMATICA to help us obtaining such equations. They are quite involved and not particularly enlightening. For our purposes, it is useful to organize these equations so that each equation has second derivatives of a single function. This is achieved by taking the following combinations of the Einstein equations: [7],

$$E_r^r + E_\theta^\theta - E_\varphi^\varphi - E_t^t = 0 \,, \tag{3.11}$$
$$E_r^r + E_\theta^\theta - E_\varphi^\varphi + E_t^t + 2W E_\varphi^t = 0 \,, \tag{3.12}$$
$$E_r^r + E_\theta^\theta + E_\varphi^\varphi - E_t^t - 2W E_\varphi^t = 0 \,, \tag{3.13}$$
$$E_\varphi^t = 0 \,, \tag{3.14}$$

where $E_\nu^\mu \equiv R_\nu^\mu - 1/2\delta_\nu^\mu \; R = 0$ are the Einstein equations. Although these 4 combinations give us four equations with second derivatives of a single of the four metric functions, another two combinations can be made to obtain two "constraint" equations that can be used to test the numerical accuracy of the solutions. Such constraint combinations are [7],

$$E_r^r - E_\theta^\theta = 0 \,, \tag{3.15}$$
$$E_r^\theta = 0 \,. \tag{3.16}$$

With the equations of motion written, we introduce a new radial variable $\bar{x} = x/(1+x)$ with the intention of mapping the semi-infinite region $[0, \infty[$ to the finite region $[0, 1]$. With such transformation we can rewrite the equations of motion with the following substitutions [7],

$$x \; \partial_x \mathcal{F} \longrightarrow (1-\bar{x})\partial_{\bar{x}} \mathcal{F} \,, \qquad x^2 \; \partial_{xx} \mathcal{F} \longrightarrow (1-\bar{x}^2)\partial_{\bar{x}\bar{x}} \mathcal{F} - 2(1-\bar{x})\partial_{\bar{x}} \mathcal{F} \,, \tag{3.17}$$

where $\mathcal{F} = \{F_0, F_1, F_2, W\}$ are the metric functions and $x = \sqrt{r^2 - r_H^2}$, as before.

Finally, we implemented these equations, together with the boundary conditions, on the FIDISOL/CADSOL solver and used the BLAFIS supercomputer to run the solver. The solver gives us, as an output, discrete values of the metric functions on a chosen grid, composed by discrete points within integration region $0 \leq \bar{x} \leq 1$ and $0 \leq \theta \leq \pi/2$ (the values for $\pi/2 \leq \theta \leq \pi$ are obtained due to the reflexion symmetry along the equatorial plane). Typical grids use 250 points in the $x-$direction and 30 points in the $\theta-$one.

The best way to compare the analytically known Kerr BH metric, henceforth dubbed *theoretical* solution, with a numerical one, obtained by the above strategy, is to compare the physical quantities of both. In the case of the theoretical Kerr BH, we must start by writing its physical quantities in the non-standard coordinate system used. Such is presented in Appendix A, together with plots of the theoretical lines of the physical quantities. On the other hand, the physical quantities of a numerical BH are encoded in terms of the metric functions, and can be obtained, either at the horizon or at infinity. Considering first the horizon quantities, we can introduce the Hawking temperature [24], $T_H = \kappa/(2\pi)$, where κ is the surface gravity, and the entropy, $S = A_H/4$ [25], where,

$$T_H = \frac{1}{4\pi r_H} e^{(F_0 - F_1)|_{r_H}} \ , \qquad A_H = 2\pi r_H^2 \int_0^\pi d\theta \sin\theta e^{(F_1+F_2)|_{r_H}} \ . \tag{3.18}$$

Also, the horizon angular velocity, Ω_H, is fixed by the horizon value of the metric function W,

$$\Omega_H = -\frac{t^2}{t\cdot\varphi} = -\left.\frac{g_{tt}}{g_{t\varphi}}\right|_{r=r_H} = W|_{r=r_H} \ , \tag{3.19}$$

but this quantity will not be computed since it is, together with the horizon radius, an input variable for the solver – *c.f.* Appendix A. Moving to the spatial infinity quantities, we have the ADM mass M and angular momentum J. Both can be read from the asymptotic behaviour of the metric functions,

$$g_{tt} = -1 + \frac{2M}{r} + \dots \ , \qquad g_{t\varphi} = \frac{2J}{r}\sin^2\theta + \dots \ . \tag{3.20}$$

In Figure 3.1 and Figure 3.2 we have the numerical points and the theoretical line of the four physical quantities mentioned before. Here we choose to vary only the horizon radius, r_H, fixing the horizon angular velocity, Ω_H. As one can see, we have two branches – *c.f.* Appendix A –, associated to two different cases when one takes the limit $r_H \to 0$: In the down branch, we arrive to a static Schwarzschild configuration; in the up branch, we arrive to an extremal Kerr configuration. Such structure of branches makes clear that for the same horizon radius (and horizon angular velocity) we have, in general, two BHs with different physical quantities, M, J. One can also see that the numerical points agree very well with the theoretical line and to get a better insight about this, we display in Figure 3.3 and Figure 3.4 the relative error of the numerical data. In these figures we can see that the errors vary between 10^{-4} and 10^{-7}, depending on the physical quantity, which is quite acceptable, and provides a good test for this solver. We can also see a general behaviour: the error always increases when we approach both limits of the horizon radius range: $r_H \to 0$ and $r_H \to r_H^{(max)}$, for both branches. In the former case, such behaviour happens because we are approaching a region where the numerics starts to become more difficult to perform, especially in the up branch where we approach extremality. Then, we are in a region where two solutions are very close to each other with almost the same physical quantities, which tends to decrease the accuracy of the solutions found by the solver.

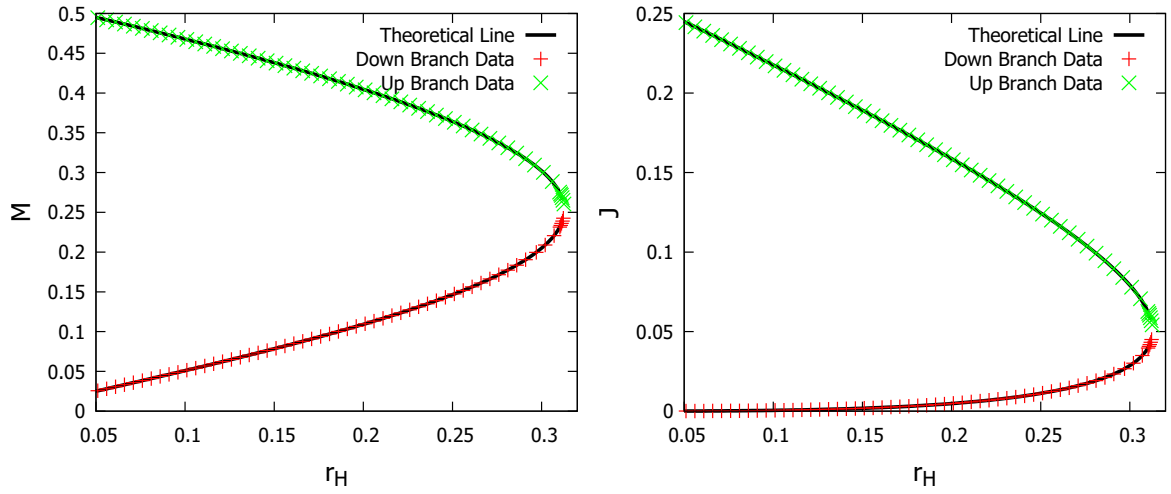

(a) (b)

Figure 3.1: The numerical data and theoretical line of the mass (a) and angular momentum (b) are displayed, for $\Omega_H = 0.96$. A very good agreement between numerical and theoretical data is visible.

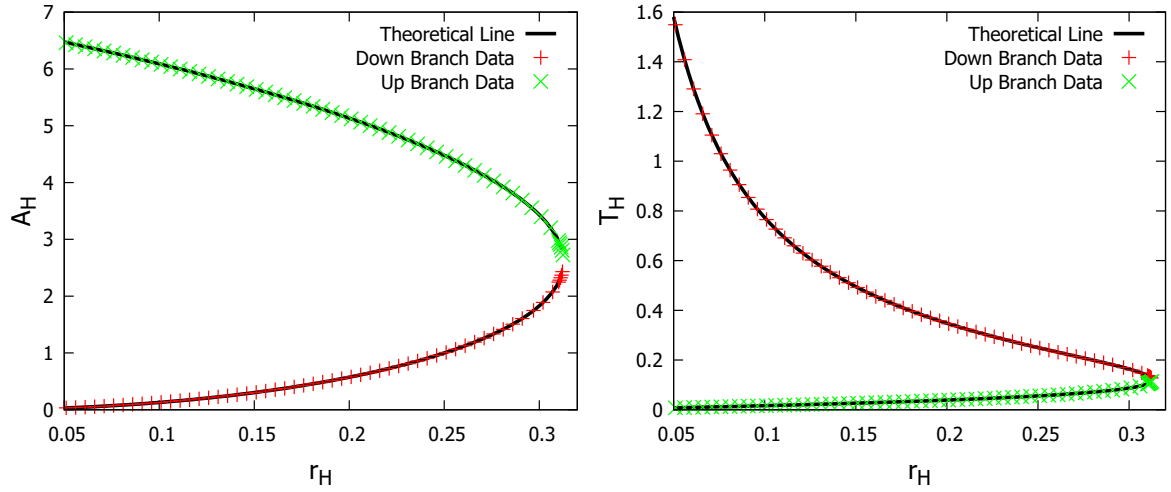

(a) (b)

Figure 3.2: The numerical data and theoretical line of the horizon area (a) and Hawking temperature (b) are displayed, for $\Omega_H = 0.96$. A very good agreement between numerical and theoretical data is visible.

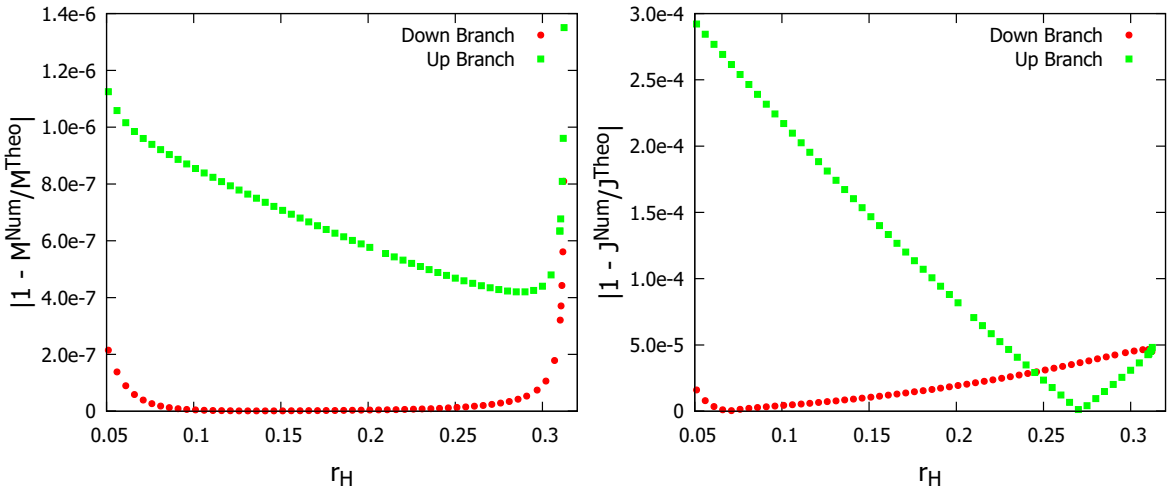

(a) (b)

Figure 3.3: Relative error of the numerical data for the mass (a) and angular momentum (b) for both branches.

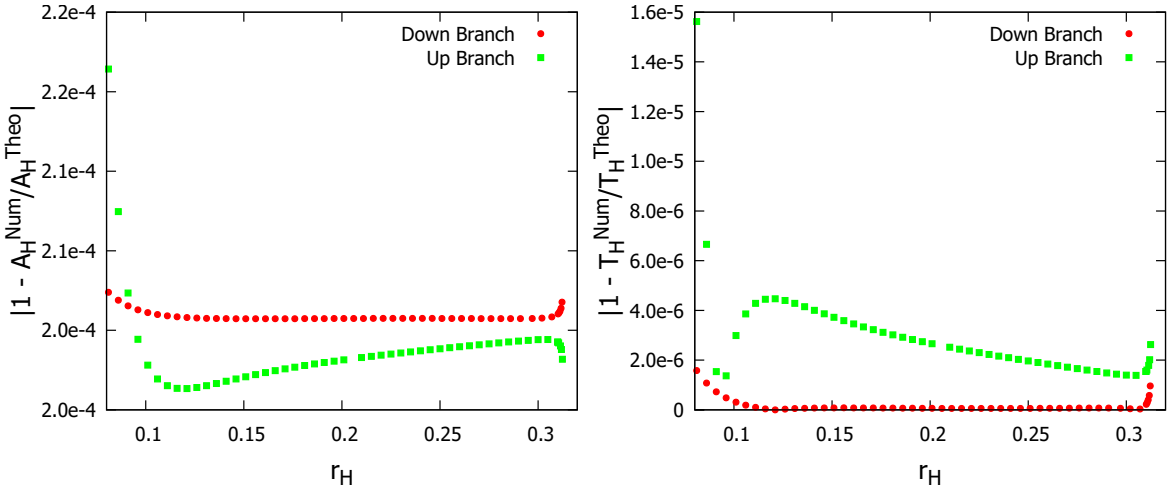

(a) (b)

Figure 3.4: Relative error of the numerical data for the horizon area (a) and Hawking temperature (b) for both branches.

Chapter 4

Physical Quantities and Bounds of a BH

In Chapter 2 we saw that the most general single BH solution of the Einstein-Maxwell equations is the KN solution and it is parameterized by its mass, M, angular momentum, J, and electrical charge, Q_E. By taking the limit $Q_E \to 0$ or $J \to 0$ one obtains the Kerr solution and the RN solution, respectively. These two solutions have a bound in their parameter space denoting an upper limit for the amount of electrical charge and angular momentum for a given mass,

$$q_E \equiv \frac{|Q_E|}{M} \leq 1 \,, \quad \text{for RN} \,, \qquad j_M \equiv \frac{|J|}{M^2} \leq 1 \,, \quad \text{for Kerr} \,; \tag{4.1}$$

when such bounds are violated, the spacetime describes a naked singularity rather than a BH.

A question one can ask is: "how fundamental are these bounds in BH Physics?". Outside the scope of strong gravity, these bounds make no physical sense since every object can violate these bounds by several orders of magnitude. For example, an electron violates the RN bound and a simple soccer ball violates the Kerr bound. But within the scope of strong gravity these bounds are reasonable because too much (one sided) electrical charge or rotation has the potential to the prevent gravitational collapse that leads to a BH. This reasoning therefore suggests that the total charge and angular momentum should be bounded by the total energy/mass in a BH spacetime, which can be seen in Equation 4.1. However, and somewhat surprisingly, Kerr BHs with scalar hair may violated the Kerr bound, both in terms of asymptotic *and* horizon quantities. This provides a new example, within a physically reasonable model, of the breakdown of the asymptotic Kerr bound.

How about the breakdown of the Kerr bound in terms of horizon quantities? Are there other examples? To tackle this question, we will discuss in this chapter the RN and Kerr bounds in terms of horizon quantities, instead of ADM ones, for the KN [12] and the Kerr-Sen [13] BHs. The latter, is a charged BH obtained in string theory, including more fields than just the standard electromagnetic field and with some non-minimal couplings, as will be described below.

This chapter is based on the paper [14], of which I am a co-author.

4.1 Horizon *vs* Asymptotic Quantities

In a stationary and axi-symmetric spacetime, the Killing symmetries allow a quasi-local definition of energy, M_S, and angular momentum, J_S, in a volume bounded by a two dimension spacelike surface S. These quantities are given by the Komar integrals [26], which take the form,

$$M_S = -\frac{1}{8\pi}\oint_S dS_{\mu\nu} D^\mu t^\nu \ , \qquad J_S = \frac{1}{16\pi}\oint_S dS_{\mu\nu} D^\mu \varphi^\nu \ , \tag{4.2}$$

where t^ν and φ^ν are the timelike and rotational Killing vectors, respectively, and $dS_{\mu\nu}$ is the surface element defined as,

$$dS_{\mu\nu} = 2n_{[\mu} l_{\nu]} \sqrt{-g} d\Omega \ , \tag{4.3}$$

in which n_μ and l_ν are the timelike and spacelike vectors normal to the surface, and $d\Omega$ is the differential solid angle.

If one takes the two dimension spacelike surface S as a 2-sphere at spacial infinity, S^2_∞, for an asymptotically flat spacetime, these quantities become the ADM ones $(M_S, J_S) \to (M, J)$; on the other hand, if one takes S as a spatial section of the event horizon, $\mathscr{H}$, these quantities become the horizon mass and angular momentum $(M_S, J_S) \to (M_H, J_H)$. An application of Gauss' theorem relates these two sets of quantities,

$$M = M_H - 2\int_\Sigma dS_\mu \left(T_\nu{}^\mu t^\nu - \frac{1}{2} T t^\mu \right) \ , \quad J = J_H + \int_\Sigma dS_\mu \left(T_\nu{}^\mu \varphi^\nu - \frac{1}{2} T \varphi^\mu \right) \ , \tag{4.4}$$

where Σ is a spacelike surface, bounded by S^2_∞ and $\mathscr{H}$. For Ricci flat spacetime, $M = M_H$ and $J = J_H$, since there will be no contribution from the energy-momentum tensor; for a non-vacuum BH spacetime, in general, these quantities differ. To measure this difference, we have found useful to define,

$$f \equiv \frac{M_H}{M} \quad \text{and} \quad h \equiv \frac{J_H}{J} \ , \tag{4.5}$$

corresponding to the fractions of ADM mass and angular momentum which are stored inside the horizon.

Another physical quantity of interest is the electric charge, which can be computed by the covariant form of Gauss' law,

$$Q_E^{(S)} = \frac{1}{8\pi}\oint_S dS_{\mu\nu} F^{\mu\nu} \ , \tag{4.6}$$

where $F^{\mu\nu}$ is the Maxwell field strength tensor, defined as $F_{\mu\nu} = \partial_\mu A_\nu - \partial_\nu A_\mu$, in which A_μ is the Maxwell 4-potential. The ADM charge, Q_E, is obtained, as before, by taking $S = S^2_\infty$, whereas the horizon charge, $Q_E^{(H)}$, is obtained by taking $S = \mathscr{H}$. These two quantities can be related by applying again the Gauss' theorem,

$$Q_E = Q_E^{(H)} + \frac{1}{4\pi}\int_\Sigma dS_\mu D_\nu F^{\mu\nu} \ , \tag{4.7}$$

thus, as expected, the two charges may differ when there are sources to Maxwell's equations outside the horizon.

4.2 Closed Form Solutions: Charged Kerr-BHs

4.2.1 Kerr-Newman BH

As seen in the Chapter 2 the configuration for a KN BH is,

$$ds^2 = -\frac{\Delta}{\Sigma}\left(dt - a\sin^2\theta d\varphi\right)^2 + \Sigma\left(\frac{dr^2}{\Delta} + d\theta^2\right) + \frac{\sin^2\theta}{\Sigma}\left[adt - \left(\Sigma + a^2\sin^2\theta\right)d\varphi\right]^2 \ , \quad (4.8)$$

$$A_\mu dx^\mu = -\frac{Q_E\ r}{\Sigma}\left(dt - a\sin^2\theta d\varphi\right) \ . \quad (4.9)$$

To address horizon quantities, we must use a regular coordinate system on the horizon, which is not the case of Boyer-Lindquist coordinates. Thus we need a coordinate system that is not singular at the horizon. For that we introduced the following coordinate transformation,

$$dv = dt + \frac{\Sigma + a^2\sin^2\theta}{\Delta}dr \quad \text{and} \quad d\psi = d\varphi + \frac{a}{\Delta}dr\,, \quad (4.10)$$

which yields the KN metric and the 1-form gauge potential in ingoing Eddington-Finkelstein-type coordinates,

$$ds^2 = -\frac{\Delta}{\Sigma}\left(dv - a\sin^2\theta d\psi\right)^2 + 2dr\left(dv - a\sin^2\theta d\psi\right) + \Sigma d\theta^2 + \\ + \frac{\sin^2\theta}{\Sigma}\left[adv - \left(\Sigma + a^2\sin^2\theta\right)d\psi\right]^2 \ , \quad (4.11)$$

$$A_\mu dx^\mu = -\frac{Q_E\ r}{\Sigma}\left(dv - \frac{\Sigma}{\Delta}dr - a\sin^2\theta d\psi\right) \ . \quad (4.12)$$

4.2.2 Kerr-Sen BH

A different type of metric, that has not been discussed in detail up to now, is the Kerr-Sen (KS) metric [13] which is a solution to the low energy effective field theory of the heterotic string, compactified on a 6-torus. In the string frame, the corresponding action is,

$$\mathcal{S} = \frac{1}{4}\int d^4x\sqrt{-G}e^{-\Phi}\left(R - \frac{1}{12}H_{\mu\nu\rho}H^{\mu\nu\rho} + G^{\mu\nu}\partial_\mu\Phi\partial_\nu\Phi - \frac{1}{8}F_{\mu\nu}F^{\mu\nu}\right), \quad (4.13)$$

where Φ is the dilation field, the Neveu-Schwarz field strength 3-form $H_{\mu\nu\rho}$ is defined as $H_{\mu\nu\rho} = 3\partial_{[\mu}B_{\nu\rho]} - 3A_{[\mu}F_{\mu\nu]}/4$, in terms of the Neveu-Schwarz 2-form potential, $B_{\mu\nu}$, and the Maxwell field strength, $F_{\mu\nu}$ and potential, A_μ. $G_{\mu\nu}$ is the string-frame metric, which is related to the Einstein-frame metric $g_{\mu\nu}$ as $g_{\mu\nu} = e^{-\Phi}G_{\mu\nu}$. Performing this conformal transformation, together with the rescalings $\Phi \to 2\Phi$ and $A_\mu \to 2\sqrt{2}A_\mu$ [27], one obtains the following Einstein-frame action,

$$\mathcal{S} = \frac{1}{4}\int d^4x\sqrt{-g}\left(R - 2\partial_\mu\Phi\partial^\mu\Phi - e^{-2\Phi}F_{\mu\nu}F^{\mu\nu} - \frac{1}{12}e^{-4\Phi}H_{\mu\nu\rho}H^{\mu\nu\rho}\right), \quad (4.14)$$

where the 3-form $H_{\mu\nu\rho}$ is now defined as $H_{\mu\nu\rho} = 3\partial_{[\mu}B_{\nu\rho]} - 6A_{[\mu}F_{\nu\rho]}$, due to the rescaled fields. The equations of motion obtained in the Einstein-frame are:

$$\Box\Phi = -\frac{1}{2}e^{-2\Phi}F_{\mu\nu} - \frac{1}{12}e^{-4\Phi}H_{\mu\nu\rho}H^{\mu\nu\rho}\,, \qquad D_\rho\left(e^{-2\Phi}F^\rho{}_\mu\right) = -\frac{1}{2}e^{-4\Phi}H_{\mu\nu\rho}F^{\nu\rho}\,, \quad (4.15)$$

$$D_\rho\left(e^{-4\Phi}H^\rho{}_{\mu\nu}\right)=0,\ ,\qquad R_{\mu\nu}-\frac{1}{2}g_{\mu\nu}R=T^{DF}_{\mu\nu}+T^{EM}_{\mu\nu}+T^{NS}_{\mu\nu}\,, \tag{4.16}$$

where the dilaton field (DF), electromagnetic (EM) and Neveu-Schwarz (NS) field energy-momentum tensor are,

$$T^{DF}_{\mu\nu}=2\left(\partial_\mu\Phi\partial_\nu\Phi-\frac{1}{2}g_{\mu\nu}\partial_\rho\Phi\partial^\rho\Phi\right)\,,\qquad T^{EM}_{\mu\nu}=2e^{-2\Phi}\left(F_{\mu\rho}F_\nu{}^\rho-\frac{1}{4}g_{\mu\nu}F_{\rho\sigma}F^{\rho\sigma}\right)\,,$$

$$T^{NS}_{\mu\nu}=\frac{1}{4}e^{-4\Phi}\left(H_{\mu\rho\sigma}H_\nu{}^{\rho\sigma}-\frac{1}{6}g_{\mu\nu}H_{\rho\sigma\lambda}H^{\rho\sigma\lambda}\right)\,.$$

One can observe, through the right equation in Equation 4.15, that in this theory the Neveu-Schwarz and the dilaton field act as sources to the Maxwell field, which contrast to the Einstein-Maxwell theory, described in Chapter 2, where there are no sources for the Maxwell field as can be seen from the right equation in Equation 2.4.

The KS configuration solves these equations of motion, and can be written in Boyer-Lindquist coordinates (t,r,θ,φ) as [27],

$$ds^2=-\frac{\Delta'}{\Sigma'}\left(dt-a\sin^2\theta d\varphi\right)^2+\Sigma'\left(\frac{dr^2}{\Delta'}+d\theta^2\right)+\frac{\sin^2\theta}{\Sigma'}\left[adt-\left(\Sigma'+a^2\sin^2\theta\right)d\varphi\right]^2\,, \tag{4.17}$$

$$A_\mu dx^\mu=-\frac{Q_E\ r}{\Sigma'}(dt-a\sin^2\theta d\varphi)\,,\qquad \Phi=-\frac{1}{2}\ln\left(\frac{\Sigma'}{\Sigma'-br}\right)\,, \tag{4.18}$$

$$B_{\mu\nu}dx^\mu\wedge dx^\nu=2a\sin^2\theta\frac{br}{\Sigma'}dt\wedge d\varphi\,, \tag{4.19}$$

where

$$\Delta'\equiv r^2-2Mr+a^2+br=\Delta-Q_E^2+br\,,\quad \Sigma'\equiv r^2+a^2\cos^2\theta+br=\Sigma+br\,,\quad b\equiv\frac{Q_E^2}{M}, \tag{4.20}$$

where Q_E is the ADM electric charge and M is the ADM mass [27].

Since we want to compute the horizon quantities we need, as before, a regular coordinate system on the horizon, which, again, is not the case of the Boyer-Lindquist-like coordinates in Equation 4.17. To obtain such a coordinate system we introduced the following coordinate transformation,

$$dv=dt+\frac{\Sigma'+a^2\sin^2\theta}{\Delta'}dr\quad\text{and}\quad d\psi=d\varphi+\frac{a}{\Delta'}dr\,, \tag{4.21}$$

which yields the line element and 1-form gauge potential,

$$ds^2=-\frac{\Delta'}{\Sigma'}\left(dv-a\sin^2\theta d\psi\right)^2+2dr\left(dv-a\sin^2\theta d\psi\right)+\Sigma' d\theta^2+$$
$$+\frac{\sin^2\theta}{\Sigma'}\left[adv-\left(\Sigma'+a^2\sin^2\theta\right)d\psi\right]^2\,, \tag{4.22}$$

$$A_\mu dx^\mu=-\frac{Q_E\ r}{\Sigma'}\left(dv-\frac{\Sigma'}{\Delta'}dr-a\sin^2\theta d\psi\right)\,. \tag{4.23}$$

As one can see, the line element of the KN metric, Equation 4.8 and Equation 4.11, the coordinate transformation, Equation 4.10, and the gauge potential, Equation 4.9 and Equation 4.12 are interchanged with those of the KS metric, Equation 4.17, Equation 4.22, the corresponding coordinate transformation, Equation 4.21, and gauge potential, Equation 4.18 and Equation 4.23, by interchanging [28]

$$(\Sigma, \Delta) \longleftrightarrow (\Sigma', \Delta') = (\Sigma + br, \Delta - Q_E^2 + br) \, . \tag{4.24}$$

4.2.3 Horizon and Asymptotic Quantities for a Kerr-Newman and Kerr-Sen BH

We will now compute the physical quantities mentioned at the beginning of this section. In order to obtain these physical quantities we used the following timelike and spacelike vectors,

$$n_\mu dx^\mu = \left(1 - \frac{a^2 \sin^2\theta}{\Sigma + a^2 \sin^2\theta}\right) dr \quad ; \quad l_\nu dx^\nu = -dv + \frac{a^2 \sin^2\theta}{2(\Sigma + a^2 \sin^2\theta)} dr \, , \tag{4.25}$$

for the KN case, and the same expression with $\Sigma \to \Sigma'$ for KS. With these vectors and the corresponding covariant derivative, one obtains the horizon mass for these two cases,

$$M_H = M \left(1 - \frac{Q_E^2}{2Mr_H}\right) \left[1 - \frac{Q_E^2}{ar_H} \arctan\left(\frac{a}{r_H}\right)\right] \, , \qquad \text{Kerr-Newman} \, , \tag{4.26}$$

$$M_H = M \left[\frac{r_H^2 + br_H/2}{r_H^2 + br_H} - \frac{Q_E^2 r_H^2}{a(br_H + r_H^2)^{3/2}} \arctan\left(\frac{a}{\sqrt{br_H + r_H^2}}\right)\right] \, , \qquad \text{Kerr-Sen} \, , \tag{4.27}$$

Proceeding similarly for the horizon angular momentum, one arrives at

$$J_H = J \left(1 - \frac{Q_E^2}{2Mr_H}\right) \left\{1 + \frac{Q_E^2}{2a^2} \left[1 - \frac{a^2 + r_H^2}{ar_H} \arctan\left(\frac{a}{r_H}\right)\right]\right\} \, , \qquad \text{Kerr-Newman} \, , \tag{4.28}$$

$$J_H = J \left[\frac{r_H^2 + 3br_H/4}{r_H^2 + br_H} + \frac{br_H}{4a^2} - \frac{Q_E^2 M r_H^3}{a^3(br_H + r_H^2)^{3/2}} \arctan\left(\frac{a}{\sqrt{br_H + r_H^2}}\right)\right] \, , \qquad \text{Kerr-Sen} \, , \tag{4.29}$$

and finally, for the horizon charge, one finds,

$$Q_E^{(H)} = Q_E \, , \qquad \text{Kerr-Newman} \, , \tag{4.30}$$

$$Q_E^{(H)} = Q_E \left[\frac{r_H^2 + br_H/2}{r_H^2 + br_H} - \frac{Q_E^2 r_H^2}{a(br_H + r_H^2)^{3/2}} \arctan\left(\frac{a}{\sqrt{br_H + r_H^2}}\right)\right] \, , \qquad \text{Kerr-Sen} \, , \tag{4.31}$$

where r_H is the radius of the event horizon, which, for the KN BH, can be written as,

$$r_H = M + \sqrt{M^2 - Q_E^2 - a^2} \, , \tag{4.32}$$

and for the KS BH is given by,

$$r_H = M - \frac{b}{2} + \sqrt{\left(M - \frac{b}{2}\right)^2 - a^2} \ . \tag{4.33}$$

Using these two equations and the fact that, $a = J/M$ and $b = Q_E^2/M$, all the physical quantities showed above can be expressed only in terms of the ADM quantities (M, J, Q_E), for both cases.

We can observe that, for both solutions,

$$\lim_{Q_E \to 0} M_H = M \ , \qquad \lim_{Q_E \to 0} J_H = J \ , \qquad \lim_{Q_E \to 0} Q_E^{(H)} = 0 \ , \tag{4.34}$$

as expected, since, in both cases, when we take the limit $Q_E \to 0$ we arrive to the Kerr solution, and it is well known in the literature [25] that a Kerr BH has its total mass and angular momentum contain within the horizon. As another consistency check, we verify the Smarr's formula [29], written solely in terms of the horizon quantities [25], that is obeyed by both KN and KS BHs,

$$M_H - 2\Omega_H J_H = \frac{\kappa A_H}{4\pi} \ , \tag{4.35}$$

where Ω_H is the angular velocity of the horizon, κ is the surface gravity and A_H is the area of the spatial sections of the event horizon. For the KN solution we have,

$$\Omega_H = \frac{a}{r_H^2 + a^2} \ , \qquad \kappa = \frac{r_H - M}{r_H^2 + a^2} \ , \qquad A_H = 4\pi(r_H^2 + a^2) \ . \tag{4.36}$$

With these results and Equation 4.26 and Equation 4.28, one can easily show that the Smarr's formula holds. For the KS solution we have,

$$\Omega_H = \frac{a}{r_H^2 + a^2 + br} \ , \qquad \kappa = \frac{r_H^2 - a^2}{4Mr_H} \ , \qquad A_H = 4\pi(r_H^2 + a^2 + br) \ . \tag{4.37}$$

These results, together with Equation 4.27 and Equation 4.29, one can, as before, show that the Smarr's formula holds.

Analysis of Horizon Quantities

To get a better insight on the results we have obtained, let us start with the KN case by mention a curious feature that occurs in the static limit ($J \to 0$) giving us the RN solution. With this limit, Equation 4.26 reduces to,

$$M_H = M - \frac{Q_E^2}{r_H} \ . \tag{4.38}$$

It can be easily interpreted that the horizon mass, M_H, is always smaller than the ADM mass, M, as expected from the fact that the electric field outside the horizon carries energy, and therefore mass. We can also interpret that the horizon mass decreases monotonically from $M_H = M$, for an uncharged BH (Schwarschild BH), to $M_H = 0$, for an extremal BH. One can see this behaviour in Figure 4.1a.

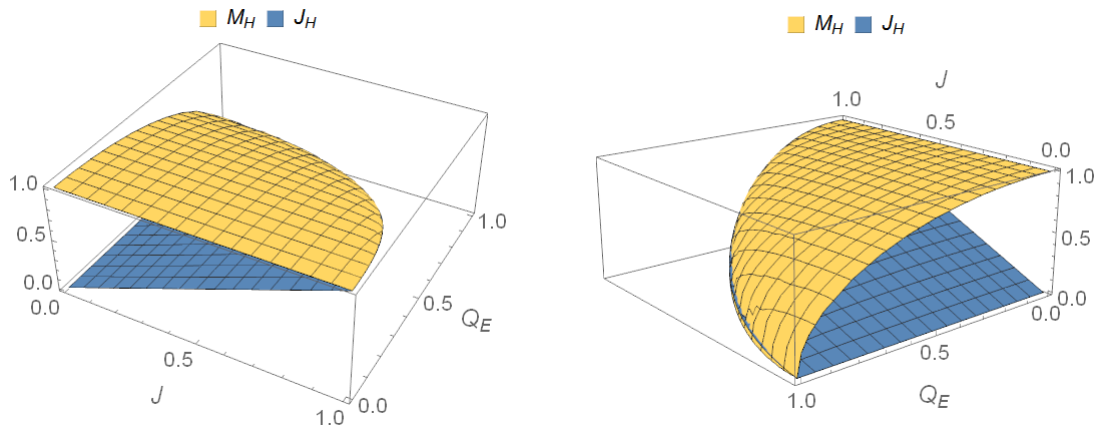

(a) (b)

Figure 4.1: Horizon mass, M_H, and angular momentum, J_H, for a KN BH in terms of its asymptotic quantities. Adapted from [14].

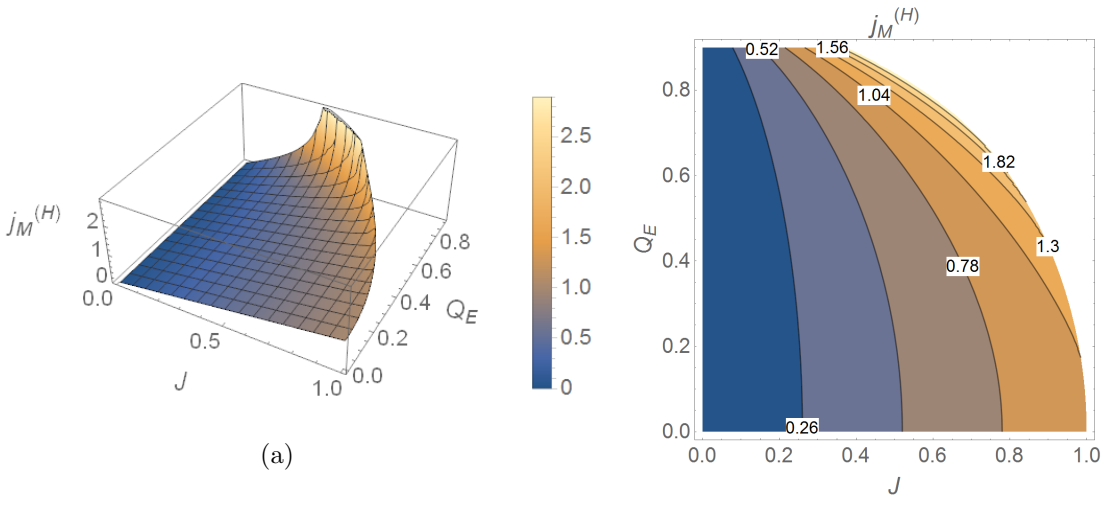

(a) (b)

Figure 4.2: (a) 3D and (b) contour plots of $j_M^{(H)} \equiv J_H/M_H^2$ for the KN BH. This quantity becomes larger than unity for sufficiently large charge and angular momentum, violating the Kerr bound. Adapted from [14].

Since for the RN BH the total charge is within the horizon, as the KN BH, we can analyse the following dimensionless quantity,

$$q_E^{(H)} \equiv \frac{\left|Q_E^{(H)}\right|}{M_H} = \frac{q_E}{\sqrt{1-q_E^2}} \,, \tag{4.39}$$

where, as seen in the beginning of this chapter, $q_E \equiv |Q_E|/M$. An immediate consequence of this quantity is that it becomes larger that unity for some values of q_E, and actually diverges when extremality is approached ($q_E \to 1$). This means that the RN bound is violated in the RN solution, in terms of horizon quantities.

To better analyse the more general KN family, let us fix the total mass, $M = 1$, (*i.e.* fix the lenght scale of the problem) and vary Q_E and J. Then:

(i) for fixed, but non-zero, J, the horizon mass M_H decreases with the increasing Q_E — similarly to the case with $J = 0$ — because a part of energy is transferred into the electric field outside the horizon — Figure 4.1b. The horizon angular momentum J_H also decreases: the growing outside electromagnetic field carries a larger fraction of the total angular momentum;

(ii) for fixed charge Q_E, by increasing the angular momentum J, the horizon angular momentum J_H will also increases, but the horizon mass M_H will decreases.

Focusing now on the Kerr bound, we recall that the existence of a event horizon in the KN metric requires $q_E^2 + j_M^2 \leq 1$, which, in particular, implies the Kerr bound $j_M \leq 1$. However, as the RN bound, this bound is strongly violate in terms of the horizon quantities. This can be seen in Figure 4.2a-Figure 4.2b. We can observe that for $Q_E = 0$, $M_H = M$ and $J_H = J$, as has been shown above in Equation 4.34, and hence the bound is valid. But for $Q_E > 0$, the bound is violated for sufficiently large values of J, but which always obey $j_M \leq 1$.

Now we turn to the KS BH. As for the KN case let us start by considering the static limit, where one finds a dilatonic charge BH. Firstly, by analysing Equation 4.33 we observe a new bound $Q_E^2/M^2 \leq 2$, which is analogous to the RN bound. Moreover, the extremal limit of the static BH is singular, *i.e.* the areal radius of the horizon vanishes. Then, from Equation 4.27 and Equation 4.31, using also Equation 4.33, we have,

$$M_H = M\left(1 - \frac{Q_E^2}{2M^2}\right) \,, \qquad Q_E^{(H)} = Q_E\left(1 - \frac{Q_E^2}{2M^2}\right) \,. \tag{4.40}$$

In the extremal limit, one concludes that both the horizon mass and charge vanish. This is consistent with the fact that the horizon area also vanishes in this limit. But the most curious features of this BH, which extends to the general family is, as can be seen from Equation 4.27 and Equation 4.31,

$$\frac{Q_E^{(H)}}{M_H} = \frac{Q_E}{M} \,. \tag{4.41}$$

Thus, the KS charge to mass ratio asymptotic bound is not violated by the horizon quantities.

In Figure 4.3 and Figure 4.4 we produce analogous plots for the KS HS to the ones in Figure 4.1 and Figure 4.2 for the KN case. The overall behaviour of all quantities is very similar to the KN case, in particular the Kerr bound can also be violated in terms of horizon

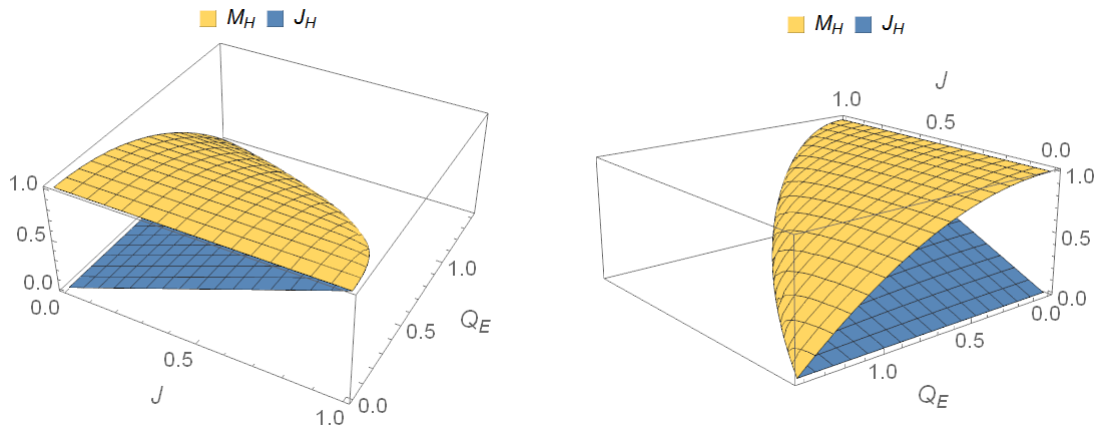

(a) (b)

Figure 4.3: Horizon mass, M_H, and angular momentum, J_H, for a KS BH in terms of its asymptotic quantities. Adapted from [14].

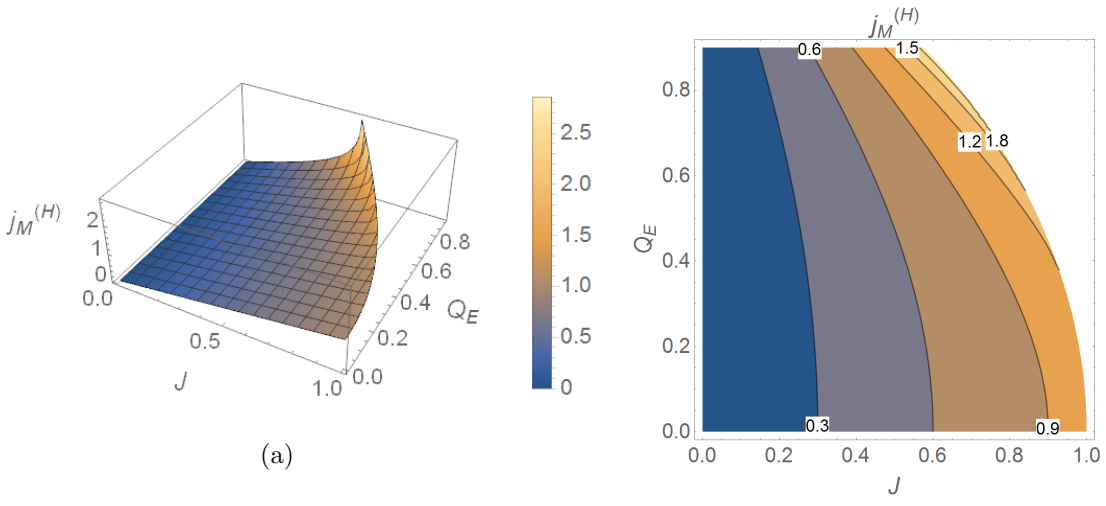

(a) (b)

Figure 4.4: (a) 3D and (b) contour plots of $j_M^{(H)} \equiv J_H/M_H^2$ for the KS BH. This quantity becomes larger than unity for sufficiently large charge and angular momentum, violating the Kerr bound. Adapted from [14].

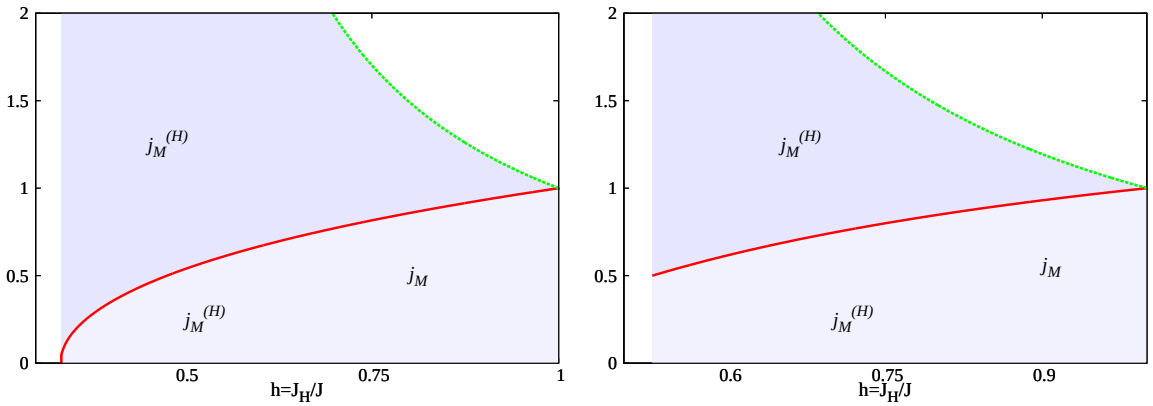

(a) (b)

Figure 4.5: Dimensionless ADM, j_M (light shaded area), and horizon, $j_M^{(H)}$ (light plus dark shaded area) angular momentum, *vs.* fraction of the angular momentum in the horizon, h for: (a) KN BHs; (b) KS BHs. In both panels, the green dashed (red solid) line corresponds to $j_M^{(H)}$ (j_M) for extremal solutions. Adapted from [14].

---

quantities — Figure 4.4. But one of the major differences is that the charge, in the KS case, can vary up to $\sqrt{2}$, whereas in the KN case only can vary up to 1.

One other way to appreciate the violation of the Kerr bound in terms of the horizon quantities for KN and KS BHs is through the fraction of horizon angular momentum that we talked in the Section 4.1, and can be seen in Figure 4.5. One can appreciate that the violations are stronger when a larger fraction of the angular momentum is outside the horizon, and as expected the ADM dimensionless angular momentum, j_M, never exceeds unity.

In Figure 4.6, we exhibit the (f, h) diagram for KN and KS BHs. This diagram shows that the charged BHs always have a larger (or equal in the vaccum Kerr limit) horizon dimensionless angular momentum, $j_M^{(H)}$, as compared to the asymptotic one, j_M. In both cases, f and h reach one, corresponding to the vacuum (Kerr) limit. But none of this solutions extends to $f, h = 0$, since there is no solitonic limit.

As one can see the Kerr and RN bounds are not so fundamental as one originally thought. But despite the (unlimited) violations of these bounds there is still a bound on the rotation as suggested in [30]. This bound is connected to the linear horizon velocity, and can be defined in the following way, for a stationary, axisymmetric BH: On the spatial sections of the event horizon one should compute the proper length L of the orbits of the $U(1)$ Killing vector field; Choosing the maximum of such proper lenghts, L_{max}, that typical occurs at the equator, one defines the circumferential radius as $R = L_{max}/2\pi$. The horizon linear velocity is simply,

$$v_H = R\Omega_H \ , \tag{4.42}$$

where Ω_H is the horizon angular velocity. It is intuitive to create the following conjecture [30]: *For stationary, axisymmetric asymptotically flat, four dimensional BH solutions, $v_H \leq c$, where c is the velocity of light, with the equality attained only for extremal vacuum Kerr.* For

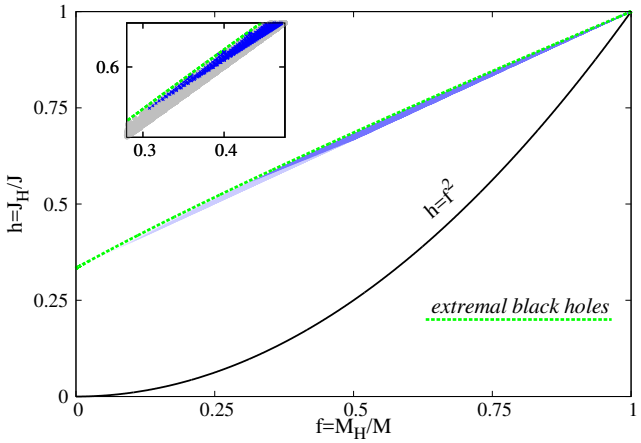

Figure 4.6: (f, h) diagrams for KN (light grey) and KS (dark blue) BHs. Adapted from [14].

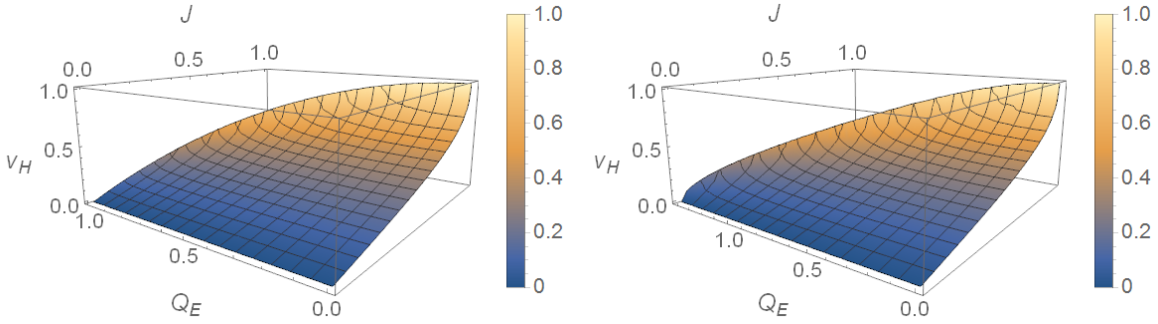

(a) (b)

Figure 4.7: Horizon linear velocity for (a) KN and (b) KS BHs. It never exceeds unity (speed of light). Adapted from [14].

---

both cases that we are studying, the linear horizon velocity can be written as follow,

$$v_H = \frac{a}{r_H}\,, \qquad \text{Kerr-Newman}\,, \tag{4.43}$$

$$v_H = \frac{a}{\sqrt{r_H^2 + b r_H}}\,, \qquad \text{Kerr-Sen}\,, \tag{4.44}$$

where, as before, $a = J/M$, $b = Q_E^2/M$ and the corresponding r_H is defined in Equation 4.32 and Equation 4.33. In Figure 4.7 we have plotted v_H in terms of the asymptotic electric charge and angular momentum. As can be observed, the horizon linear velocity bound is verified since it is always smaller than the speed of light, and only equal in the case of a vacuum extremal Kerr.

Chapter 5

Hairy BHs

It is widely accepted in the scientific community that the final outcome of the gravitational collapse of a massive star is a BH. The *uniqueness theorems* [3, 31] tell us that in electrovacuum BHs are described by the most general regular, single BH solution of the Einstein-Maxwell equations: the Kerr-Newman metric. This means that two BHs with the same mass, angular momentum and electric charge would be *exactly* identical, as opposed to other celestial bodes. These theorems led to the famous *no-hair conjecture* [5], that states that the outcome of gravitational collapse in the presence of any type of matter-energy is a KN BH, completely described by its mass, angular momentum and electric charge, in which every physical quantity can be measured asymptotically through a Gauss law, and no other physical quantities should exist. In other words, following J. Wheeler's "mantra": '*BHs have no-hair*'.

Due to this conjecture, new BH solutions that possess either new global charges (*primary hair*) or new non-trivial fields, that could be dependent on the standard global charges (*secondary hair*), that were not associated to a Gauss law, were generically referred to as 'hairy BHs'. One type of these new BHs considers one of the simplest types of matter known to physicists, a *scalar field*. Besides being one of the simplest, there exists strong observational evidence for the existence of this field in nature with the recent discovery of a scalar particle at the Large Hadron Collider, at CERN, identified as the standard model Higgs boson [32, 33]. This gives a strong motivation to study this type of field. Furthermore, scalar fields are vastly studied in the cosmological context, in an attempt to model dark energy and dark matter. Another motivation for its study is the fact that canonical scalar fields can be modeled as perfect fluids with some equation of state [34], thus can be considered as an approximation to realistic matter.

With all these motivations behind scalar fields, we will study what happens when one tries to add a scalar field to a known BH solution. In particular, in the following two chapters, such solutions are the Kerr and KN, respectively.

This chapter is based in the following papers, [6, 7, 35].

5.1 No-Scalar-Hair Theorems

Despite being a well motivated problem, physicists could not find BHs with physically reasonable scalar hair (and no gauge fields) for many years, and many thought it impossible to have such kind of BHs. Some theorems were developed to prove just assumption, one of the most influential being the one developed by Benkenstein [36, 37]. This theorem proves the

nonexistence of scalar hair surrounding a BH subject to some generic assumptions [36, 37].

5.1.1 Bekenstein's Theorem

Let us consider a rotating, stationary, asymptotically flat BH spacetime that obeys the null energy condition. From Hawking's rigidity theorem we know that this spacetime is axisymmetric and that the spatial sections of the horizon are topologically spheres [38]. In order to make these symmetries manifest, we write the spacetime metric in the following coordinates (t, r, θ, φ), so that the two Killing vectors fields read $t^\alpha \partial_\alpha = \partial_t$ and $\varphi^\alpha \partial_\alpha = \partial_\varphi$.

Let us also make the following assumptions [35]:

1. *The scalar field is canonical and is minimally coupled with Einstein's gravity*, so that the action reads,

$$\mathcal{S} = \frac{1}{4\pi} \int d^4x \sqrt{-g} \left(\frac{R}{4} - \frac{1}{2} \partial_\alpha \Psi \partial^\alpha \Psi - V(\Psi) \right) , \tag{5.1}$$

   where $V(\Psi)$ is a potential that only depends on the scalar field (This theory is dubbed *V-scalar-vacuum*). Varying the action with respect to the scalar field we obtain the (possibly non-linear) Klein-Gordon (KG) equation,

$$\Box \Psi - V'(\Psi) = 0 , \tag{5.2}$$

   where the prime denotes derivative with respect to the argument.

2. *The scalar field inherits the spacetime symmetries.* In other words, for the coordinate that we choose above, we can write,

$$\partial_t \Psi = \partial_\varphi \Psi = 0 . \tag{5.3}$$

3. *The potential obeys* $\Psi V' \geq 0$ *everywhere.* As an example we can consider the standard non-self-interacting massive scalar field potential $V(\Psi) = 1/2 \mu^2 \Psi^2$, in which one easily sees that this assumption stays true for any value of Ψ.

With these three assumptions in consideration, one can start by multiply the KG equation, Equation 5.2, by Ψ and integrate it over the BH exterior spacetime, obtaining,

$$- \int d^4x \sqrt{-g} \left(\partial_\alpha \Psi \partial^\alpha \Psi + \Psi V' \right) + \int_{\mathscr{H}} d^3\sigma n^\alpha \Psi \partial_\alpha \Psi = 0 , \tag{5.4}$$

where the boundary term is computed on the horizon, $\mathscr{H}$, and the boundary term computed at infinity vanished due to the fact that the scalar field should vanish (or at least diminish sufficiently fast) at infinity to guarantee asymptotic flatness. But, after close inspection of the horizon's boundary term, we concluded that this term must also vanish, because the event horizon of a stationary, asymptotically flat spacetime is a Killing horizon, thus, the normal vector to the horizon, n^α, is a linear combination of the Killing vector fields, and since, by Assumption 2, the scalar field is invariant under this vector field, $n^\alpha \partial_\alpha \Psi = 0$. We conclude that,

$$\int d^4x \sqrt{-g} \left(\partial_\alpha \Psi \partial^\alpha \Psi + \Psi V' \right) = 0 . \tag{5.5}$$

Through Assumption 3 we know that the second term of the previous equation is non-negative and, again by Assumption 2, one can easily prove that the gradient of the scalar field is orthogonal to both Killing vectors and thus must be spacelike or null, which means that $\partial_\alpha \Psi \partial^\alpha \Psi \geq 0$. Therefore Equation 5.5 holds if and only if $\Psi = 0$, proving that a rotating, stationary, axisymmetric and asymptotically flat BH cannot support a V-scalar field.

5.1.2 Violation of the Bekenstein's Theorem

As for any other physical or mathematical theorem, they are based in assumptions, and when one or more of these assumptions are violated, the result of the theorem may or may not hold. In fact, violating one of the assumptions of the Bekenstein's theorem does not guarantee, by itself, the existence of a regular BH with scalar hair. But we will see that the violation of the Assumption 2 will open a door to a new and exciting universe of solutions of regular, stationary and asymptotically flat BHs with scalar hair [1].

Assumption 2 is, maybe, the most straightforward and natural assumption to make in this problem, since the geometry has a set of symmetries. But imposing the same symmetries for the scalar field as those of the geometry is not essential. Through Einstein equations we understand that if the geometry have some symmetry, then the energy-momentum tensor must also have those symmetries. This is the crucial part. We can have a scalar field that *does not have* the symmetries of the geometry, and yet have a energy-momentum tensor with the same symmetries as the geometry. This can be achieved by allowing the scalar field to be complex and to possess a harmonic time dependence, $\Psi \propto e^{-i\omega t}$. This form of Ψ allows the energy-momentum tensor to be time-independent, even though the scalar field is time dependent; hence it is compatible with static and spherically symmetric geometries, and can allow the existence of solutions with scalar hair.

One example of this type of solutions, albeit not BHs, are bosons stars (BSs) [8, 39]. These exotic stars are self-gravitating, solitonic-like, scalar field configurations, which have a potential of the form $V(\Psi) = 1/2\mu^2\Psi^2 + \ldots$, where μ is the mass of the field and '...' correspond to higher order terms on the scalar field (*e.g.*, terms describing self-interactions). They were first discussed by Kaup [40] in 1968, and one year later by Ruffini and Bonazzola [41]. Since these object are not BHs, one can ask if these objects possess BH generalizations and as we will see in the next section they indeed possess a BH generalization: *Kerr BHs with scalar hair*.

5.2 Kerr BHs with Scalar Hair

Kerr BHs with scalar hair (KBHsSH) are regular (on and outside an event horizon), stationary, axisymmetric and asymptotically flat spacetimes, that violate the Assumption 2 in a similar fashion as describe above for BSs. The corresponding action is,

$$\mathcal{S} = \frac{1}{4\pi} \int d^4x \sqrt{-g} \left(\frac{R}{4} - \partial_\alpha \Psi^* \partial^\alpha \Psi - \mu^2 \Psi^* \Psi \right) . \tag{5.6}$$

[1] Violations of the other 2 assumptions can be also performed and one can obtain hairy solutions that way, but such solutions involve endowing the scalar field with some non-trivial dynamics due to either some (often unphysical) self-interactions or some tricky modification of the coupling to gravity. For a review about these different solutions, see the paper [35].

which yield the following equations of motion,

$$R_{\alpha\beta} - \frac{1}{2} g_{\alpha\beta} R = 2T_{\alpha\beta} \ , \qquad \Box\Psi = \mu^2 \Psi \ , \tag{5.7}$$

where $T_{\alpha\beta}$ is the energy-momentum tensor associated with the scalar field and is written as,

$$T_{\alpha\beta} = 2\partial_{(\alpha}\Psi^* \partial_{\beta)}\Psi - g_{\alpha\beta}\left(\partial_\gamma \Psi^* \partial^\gamma \Psi + \mu^2 \Psi^* \Psi\right) \ . \tag{5.8}$$

The energy-momentum tensor must be compatible with the background symmetries of a stationary BH. But that does not require the scalar field to be time independent. Indeed, the scalar field can be time and azimuthal dependent in such a way that one can write the scalar field as,

$$\Psi = \phi(r, \theta) e^{-i\omega t} e^{im\varphi} \tag{5.9}$$

(see below for the meaning of notation in Equation 5.9). In this way the energy-momentum tensor is compatible with the symmetries of a stationary (and axisymmetric) BH.

5.2.1 Linearised analysis: *Scalar Clouds*

The best way to approach a non-linear problem like this one is by starting with the linear approximation to get a better insight. With this in mind we linearise the equations of motion on the scalar field, Equation 5.7, and obtain

$$R_{\alpha\beta} = 0 \ , \qquad \Box\Psi = \mu^2 \Psi \ . \tag{5.10}$$

From this result one can understand that we have a massive scalar field on a background vacuum solution of Einstein's equations. In particular, we choose that vacuum solution to be the Kerr solution.

As we saw above, a scalar field of the form of Equation 5.9 circumvents the assumptions of Bekenstein's theorem yielding the hope that we can construct regular, stationary and asymptotically flat BHs. So, it is perfectly reasonable to use that scalar field as our ansatz. Then, in BL coordinates, (t, r, θ, φ), the Klein-Gordon equation can be separated as

$$\Psi = R_{lm}(r) S_{lm}(\theta) e^{-i\omega t} e^{im\varphi} \ , \tag{5.11}$$

where ω is the frequency, $m \in \mathbb{Z}$ is the azimuthal quantum number, S_{lm} are the spheroidal harmonics with $-l \leq m \leq l$ and R_{lm} satisfies a radial Teukolsky equation [6, 42],

$$\left(\Delta R'_{lm}\right)' = \left(a^2\omega^2 - 2ma\omega + \mu^2 r^2 + A_{lm} - \frac{K^2}{\Delta}\right) R_{lm} \ , \tag{5.12}$$

where the prime denotes the radial derivative, $\Delta = r^2 - 2Mr + a^2$, $K \equiv (r^2 + a^2)\omega - am$ and A_{lm} is a separation constant. One may then search for bound-state type solutions of this last equation, with the requirement that this solution, which only depends on r, decays exponentially. Due to the fact that we must impose a purely ingoing boundary condition on the horizon (in a co-rotating frame), such solutions, generically, only yield *quasi-bound* states which have a complex frequency, $\omega = \omega_R + i\omega_I$, rather than just a real one. In the case of a Schwarzschild background, one finds that all solutions have a negative complex frequency $\omega_I < 0$, therefore $\Psi \propto e^{-|\omega_I| t} e^{-i\omega_R t}$, which means that the amplitude of the scalar field decays over time, thus falling to the BH [43]. The same happens for the Kerr case if $\omega_R > m\Omega_H$,

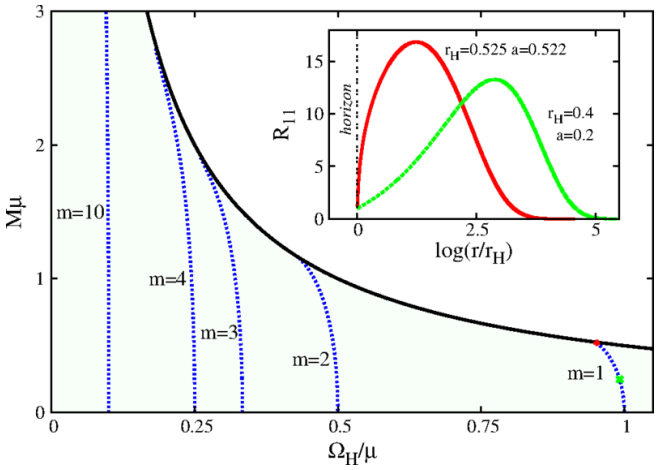

Figure 5.1: (M, Ω_H) diagram for Kerr BHs. The shaded region correspond to the existence domain of Kerr BHs, which are bounded by a solid black line, coinciding with the extremal BHs, which obey $M = 1/(2\Omega_H)$. Five existence lines are shown, for $n = 0$, $l = m$ and different m's. (Inset) $R_{lm}(r)$ for $m = l = 1$, normalized such that $R_{11}(r_H) = 1$. The two cases in this inset corresponding to the two point mark in the main panel, with its respective colour. Adapted from [6].

---

where Ω_H is, as before, the horizon's angular velocity. In the opposite case, when $\omega_R < m\Omega_H$, the complex part of the frequency becomes positive, $\omega_I > 0$, therefore $\Psi \propto e^{|\omega_I|t} e^{-i\omega_R t}$, which means that the amplitude of the scalar field increases over time, thus escaping the BH. This is due to the phenomenon of *superradiance* [35, 44]: the scalar field can be amplified in a scattering process with a Kerr BH, by virtue of extracting rotational energy from the BH.

Although only quasi-bound states are possible in these two regimes, Hod showed that true bound states exist at the threshold of superradiance [45, 46], *i.e.*, when

$$\omega = m\Omega_H \ . \tag{5.13}$$

This is known as the *synchronization condition*. At this frequency, the imaginary part of the frequency vanishes, $\omega_I = 0$, therefore $\Psi \propto e^{-i\omega_R t}$, which means that the amplitude of the scalar field is now only proportional to an harmonic term which oscillates between two complex numbers, thus yielding a true bound state. Such bound states are dubbed *scalar clouds* [6, 45, 46, 47, 48] . They form a discrete set labelled by 3 'quantum' numbers, (n, m, l), where n is a non-negative integer, corresponding to the node number of R_{lm}.

If one fixes the three 'quantum' numbers (n, m, l), one finds a 1-parameter subspace of the 2-dimensional Kerr parameter space, the *existence line*. In Figure 5.1 we show such lines in a (M, Ω_H) diagram, for fundamental nodes, $(n = 0)$, with $l = m$ and several values of m. It is important to mention that since scalar clouds lie precisely at the threshold of the superradiance instability, all solutions to the right of a given existence linear contains unstable Kerr solutions against the corresponding node. Additionally, existence lines for nodes with a given m and $l > m$ always lie to the right of the line for $m = l$, which means they are unstable. Thus, the line with $m = l$ defines the threshold of the instability for a given m.

5.2.2 The Non-Linear Setup

Due to the linear approximation held in the previous subsection, we now have a better understanding of this problem. But, in order to achieve full understanding, we have to solve the non-linear equations of motion, Equation 5.7. For this purpose, we used the solver described in Chapter 3, in which we used, for the scalar field, the same ansatz as for the scalar clouds (without separating variables), Equation 5.9 and, since we have to solve the Einstein equations and the solution has to be regular, stationary and asymptotically flat, we used, for the metric, the same ansatz as in Section 3.1,

$$ds^2 = -e^{2F_0} N dt^2 + e^{2F_1}\left(\frac{dr^2}{N} + r^2 d\theta^2\right) + e^{2F_2} r^2 \sin^2\theta (d\varphi - W dt)^2 \ , \tag{5.14}$$

with $N = 1 - r_H/r$ and where $F_i, W, i = 0, 1, 2$, are functions of r and θ only. We remember that this metric is not in Boyer-Lindquist coordinates, as mentioned in Section 3.1 (see also Appendix A).

One can observe that the metric ansatz has two Killing vector fields, $t^\alpha \partial_\alpha = \partial_t$ and $\varphi^\alpha \partial_\alpha = \partial_\varphi$, which is compatible with stationarity. However, these two Killing vector fields do not generate symmetries of the full solution, since they not preserve the expression of the scalar field, as we discussed in the previous section. The only symmetry of the full solution is generated by a linear combination of these two Killing vector fields, known as the helicoidal vector field,

$$\epsilon^\alpha = t^\alpha + \frac{\omega}{m}\varphi^\alpha \ , \tag{5.15}$$

This vector field is very reminiscent of the null horizon generator for rotating BHs, $\xi^\alpha = t^\alpha + \Omega_H \varphi^\alpha$, and indeed is the same, because of the synchronization condition, Equation 5.13. This guarantees that the null geodesic generators of the horizon are tangent to the Killing vector field ϵ^α. The physical significance of such identification is that there is no flux of scalar field into the BH,

$$\epsilon^\alpha \partial_\alpha \Psi = 0 \ . \tag{5.16}$$

In order to perform the numerical integration of the equations of motion, appropriate boundary condition must be imposed. Since this problem is a generalization of the Kerr solution, and we already obtain numerically that solution in Section 3.1, is quite natural to use the same boundaries and the same logic that was used for that case. Thus the boundary conditions for the metric functions are similar to those give in Section 3.1. But for KBHsSH we also have the scalar field, so we must specify also the boundary condition for the scalar field:

(i) *Asymptotic boundary conditions.* Asymptotically flatness implies that the solution must converge to a Minkowski spacetime at spatial infinity, thus,

$$\lim_{r\to\infty} \phi = 0 \ . \tag{5.17}$$

Furthermore, the asymptotic behaviour of the scalar field must agree with the linear analysis [6]: $\phi = f(\theta) e^{-\sqrt{\mu^2-\omega^2} r}/r + ...$ Thus, bound states require $\omega < \mu$.

(ii) *Axis boundary conditions.* Axial symmetry and regularity imply that the scalar field must vanishes at the poles, *i.e.* at $\theta = 0, \pi$,

$$\phi|_{\theta=0,\pi} = 0 \ . \tag{5.18}$$

Also, due to the symmetry with the equatorial plane we can impose the following boundary condition on the equatorial plane,

$$\partial_\theta \phi|_{\theta=\pi/2} = 0 \, . \tag{5.19}$$

(iii) *Event horizon boundary conditions.* As in Section 3.1, we can make a coordinate transformation in the form, $x = \sqrt{r^2 - r_H^2}$ to simplify the numerical treatment, and with this new coordinate one can compute a power series expansion near the horizon, $x \to 0$, of the scalar field,

$$\phi = \phi_0(\theta) + \mathcal{O}(x^2) \, , \tag{5.20}$$

With this result it is natural to impose the following boundary condition,

$$\partial_x \phi|_{r=r_H} = 0 \, . \tag{5.21}$$

5.2.3 Physical Quantities

As we have seen in Chapter 4, an axisymmetric and stationary spacetime, such as the metric Equation 5.14, guarantees the existence of two conserved global charges, the total mass M and angular momentum J, which can be computed either as Komar integrals at spatial infinity or from the decay of the appropriate metric function, as seen before in Equation 3.20.

These quantities can be split into the horizon contribution – computed as a Komar integral on the horizon, Equation 4.2 where one takes S as a spatial section of the event horizon, $\mathscr{H}$ – and the scalar field contribution computed as the volume integrals of the energy-momentum tensor components,

$$M = M^\Psi + M_H \, , \qquad J = J^\Psi + J_H \, , \tag{5.22}$$

where M_H and J_H are, as before, the horizon mass and angular momentum. M^Ψ and J^Ψ are the scalar field energy and angular momentum outside the horizon, with,

$$\begin{aligned} -M^\Psi &= \int_\Sigma dS^\alpha \left(2T^\Psi_{\alpha\beta} t^\beta - T^\Psi t_\alpha \right) = \\ &= 4\pi \int_{r_H}^\infty dr \int_0^\pi d\theta \; r^2 \sin\theta e^{F_0+2F_1+F_2} \left(\mu^2 - 2e^{-2F_0} \frac{\omega(\omega - mW)}{N} \right) \phi^2 \, , \end{aligned} \tag{5.23}$$

while $J^\Psi = mQ$, where Q is the Noether charge associated with the *global* $U(1)$ symmetry of the complex scalar field,

$$Q = \int_\Sigma d^3x \sqrt{-g} j^t = 4\pi \int_{r_H}^\infty dr \int_0^\pi d\theta \; r^2 \sin\theta e^{-F_0+2F_1+F_2} \frac{\omega - mW}{N} \phi^2 \, , \tag{5.24}$$

where j^t is the time component of the conserved current $j^\alpha = -i \left(\Psi^* \partial^\alpha \Psi - \Psi \partial^\alpha \Psi^* \right)$ associated to the *global* $U(1)$ symmetry of the scalar field. To have a better understanding of how hairy the BH is, it is convenient to introduce the normalized Noether charge,

$$q \equiv \frac{mQ}{J} \, , \tag{5.25}$$

with $q = 1$ for boson stars, which obey $J = mQ$ [49, 50], and $q = 0$ for Kerr BHs. Also the BH horizon introduces a Hawking temperature and a horizon area, Equation 3.18, where the latter is related to the BH entropy by $S = A_H/4$.

Most of these quantities are related to each other by the following Smarr formula [6, 7],

$$M = 2T_H S + 2\Omega_H (J - mQ) + M^{\Psi} \tag{5.26}$$

and by the 1st law of black holes thermodynamics,

$$dM = T_H dS + \Omega_H dJ \ . \tag{5.27}$$

One can, by adding together Equation 5.22 and Equation 5.26, also recover the same horizon's Smarr formula, Equation 4.35,

$$M_H = 2T_H S + 2\Omega_H J_H \ . \tag{5.28}$$

5.2.4 The Results

When dealing with gravitating massive scalar field, it is usual and convenient to perform the numerical integration with dimensionless variables, which are introduced by using natural units set by μ and G [7],

$$r \to r\mu \ , \qquad \phi \to \phi M_{Pl}/\sqrt{4\pi} \ , \qquad \omega \to \omega/\mu \ , \tag{5.29}$$

where $M_{Pl}^2 = G^{-1}$ is the Planck mass. As a result, all equations will be independent of both μ and G, but the global charges and all other quantities will be expressed in units set by μ and G. Since we already set $G = 1$ in Chapter 2 by using natural units, all the quantities will be only expressed in units set by the mass of the scalar field, μ.

The best way to show the results that we obtained is by examining Figure 5.2a, where we have the domain of existence of KBHsSH, obtained by extrapolating into the continuum the results from a discrete set of thousands of numerical solutions. We can see that, for $q = 0$, we recover the existence line (dotted blue line) that we talked about in Subsection 5.2.1, which represent the line of existence of Kerr BH with scalar clouds, with $m = l = 1$. In the opposite case, when $q = 1$ (red solid line), r_H vanishes, leaving only the self-gravitating scalar field, which is in fact a boson star. This proves that KBHsSH, not only are the non-linear realization of the scalar clouds obtained before, but are also the BH generalization of bosons stars. Thus, they connect bosons stars with Kerr BHs supporting scalar clouds. One can also see that the boson star line spirals inwards into a small central region, where numerics become increasingly challenging, yielding several branches of solutions. One final line that delimits the domain of existence corresponds to the extremal KBHsSH, *i.e.*, solutions where the Hawking temperature vanishes. A similar picture can be found for other values of m.

In Figure 5.2b we have the same domain of existence but now in a ADM (J, M) diagram. We have again the extremal Kerr line (solid black line), where Kerr BHs lie above such line, the boson star line, $q = 1$, represented by the solid red line, the Kerr limit, $q = 0$, imprint as the dotted blue line, and KBHsSH populate the blue shaded area. As one can observe KBHsSH can violate the Kerr bound, j_M in Equation 4.1, since there are solutions below the black solid line. This result is not that surprising, since it is known that BSs can violate this bound [51], and since, as we saw, KBHsSH are the BH generalization of BS, then it is quite natural to expect the same to occur for KBHsSH, at least for solutions with q close to unity, and that is what we see in Figure 5.2a. A second observation can be made by looking to the region where exist both Kerr BHs and KBHsSH. In such region, a KBHSH has the exact same mass and angular momentum as a Kerr BH, creating a region of *non-uniqueness*, because M

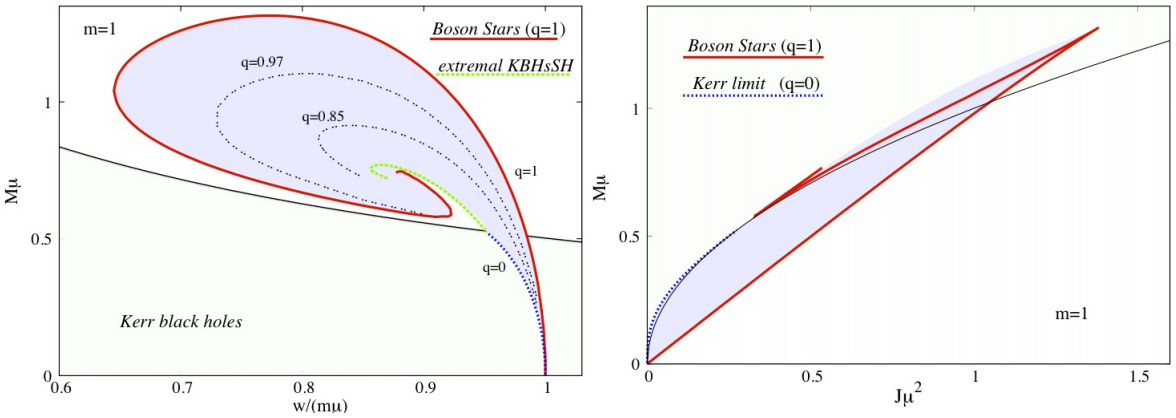

(a) (b)

Figure 5.2: (a) The (Ω_H, M) domain of existence of KBHsSH for $m = 1$ (shaded blue region), with the extremal Kerr BH line (solid black line) and Kerr limit (dotted blue line). (b) The (J, M) domain of existence of KBHsSH for $m = 1$ (shaded blue region) with the extremal Kerr BH line (solid black line), where Kerr BHs exist above that line. Adapted from [7].

---

and J are the only asymptotic charges. However, by specifying q the degeneracy seems to be completely erased [7]. In this way each BH has a unique set of charges (M, J, q). One last observation, best viewed in Figure 5.2a, is that there is a lower bound for the horizon angular velocity set by the minimal value of the scalar field frequency. This shows that KBHsSH do not possess a static limit, as opposed to the bald case, which agrees with the work done in [52].

In Figure 5.2, all the global quantities are the ADM ones. One can ask what happens when we use the horizon quantities instead of the ADM ones, namely if the Kerr bound is also violated in terms of horizon quantities. With this in mind, we plot Figure 5.3a, where we have the dimensionless ADM angular momentum, $j_M = J/M^2$, the dimensionless horizon angular momentum, $j_M^{(H)} = J_H/M_H^2$, and the fraction of angular momentum in the horizon, $h = J_H/J$ – quantities already introduced in Chapter 4. We can see, as before, that the Kerr bound is violated in terms of ADM quantities, but we also see that these solutions violate the Kerr bound in term of horizon quantities. We additionally plot Figure 5.3b, where $f = M_H/M$ is the fraction of the mass in the horizon, to show that is possible to obtain solutions with a dimensionless horizon angular momentum, $j_M^{(H)}$, greater than the ADM one, j_M, corresponding to solutions above the solid black line, $h = f^2$. In contrast, solutions with $j_M^{(H)} < j_M$ correspond to solutions below the $h = f^2$ line.

In the non-uniqueness region, we can have Kerr BHs and KBHsSH with the exact same mass and angular momentum, and one can only distinguish them with the normalized Nother charge, q. Since in this region both BHs can exist, one may wonder which one of them is more entropically favoured. To answer that question, we exhibit, in Figure 5.4, the area of the horizon as a function of J along constant M curves. In the non-uniqueness region we can show that the KBHsSH always have large values of horizon's area than the Kerr BHs, for the same M and J, meaning that the former have large entropies than the latter, thus being impossible to decay adiabatically to Kerr BHs, since they are entropically favoured.

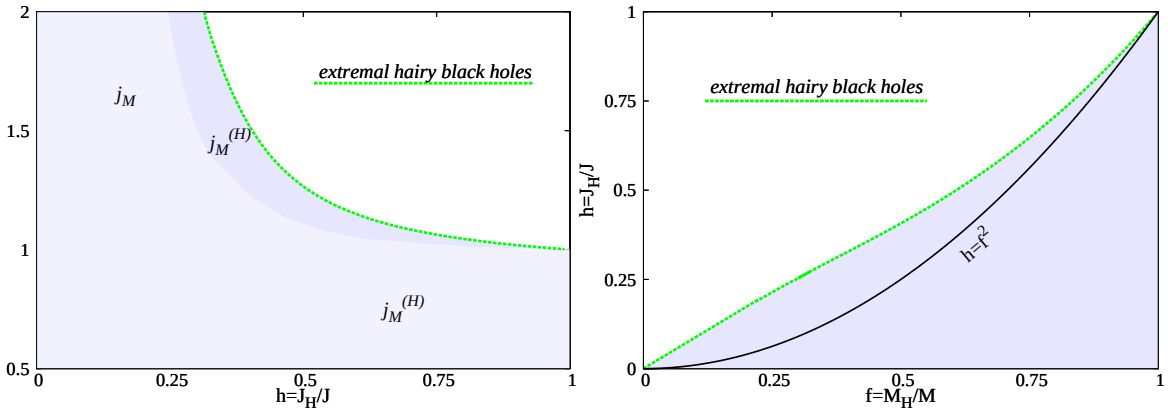

(a) (b)

Figure 5.3: (a) Dimensionless ADM, j_M (light shaded area), and horizon, $j_M^{(H)}$ (light plus dark shaded area) angular momentum, *vs.* fraction of the angular momentum in the horizon, h. (b) Fraction of angular momentum in the horizon, h, *vs.* fraction of the mass in the horizon, f. Solution above the black solid line have a horizon dimensionless angular momentum larger than the ADM one. In both panels, the dotted green line corresponds to extremal KBHsSH. Adapted from [14].

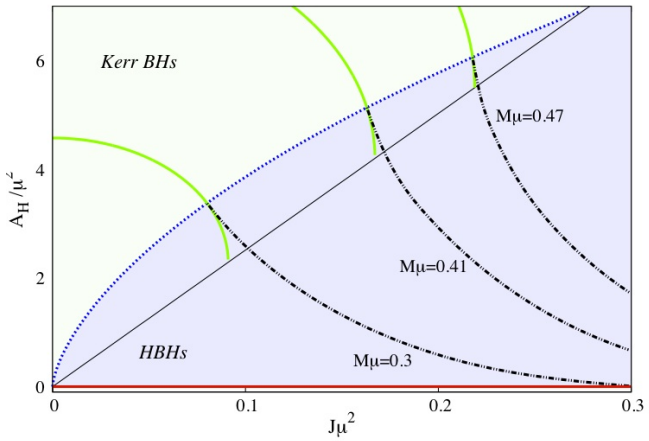

Figure 5.4: Domain of existence of KBHsSH (shaded blue region) in a (J, A_H) diagram. Kerr BHs exist above the solid black line (extremal Kerr BHs) as KBHsSH exist below the dotted blue line (Kerr limit, $q = 0$). The red solid line, as before, correspond to BSs, $q = 1$. The solid green and black dotted lines are lines with constant mass M for Kerr BHs and KBHsSH, respectively, connecting both in the Kerr limit. In the uniqueness region – above the black solid line and below the dotted blue line – the KBHsSH always have larger area for the same M and J. Adapted from [7].

Chapter 6

Kerr-Newman BHs with Scalar Hair

In 1965, Erza Newman and his colleagues presented a new analytic solution of the Einstein Equations [12], in which they generalized the Kerr solution [4] by adding electric charge to a rotating BH, yielding the famous KN solution, Equation 2.8 and Equation 2.9. In this chapter the same idea will be implemented. We will start with KBHsSH, discussed in the previous chapter, and add, firstly, electric charge only to the BH, giving a configuration in which we have a KN BH with ungauged scalar hair (KNBHUSH). Then we will add electric charge to the scalar hair too, returning a KN BH with gauged scalar hair (KNBHGSH).

Although the astrophysical interest of these new solutions is more limited compared to the solutions of the previous chapter, due to efficient discharge mechanisms (a discussion about this can be found in [53]), understanding their existence and their physical properties is of relevance to fully grasp the impact of this scalar (or other) hair on the paradigmatic BHs of GR.

This chapter is based on the paper [16], recently published, of which I am a co-author.

6.1 Ungauged Scalar Field Model

6.1.1 Action, Equations of Motion and Ansatz

We start by considering Einstein-Maxwell theory, minimally coupled to a complex, massive (mass μ) ungauged scalar field Ψ, yielding the Einstein-Klein-Gordon-Maxwell action. This action can be written as,

$$\mathcal{S} = \frac{1}{4\pi}\int d^4x\sqrt{-g}\left[\frac{R}{4} - \frac{1}{4}F_{\alpha\beta}F^{\alpha\beta} - \partial_\alpha\Psi^*\partial^\alpha\Psi - \mu^2\Psi^*\Psi\right] , \tag{6.1}$$

where, as before, $F_{\alpha\beta}$ are the components of the Maxwell 2-form, F. The Einstein-Klein-Gordon-Maxwell equations, obtained by varying the action with respect to the metric, scalar field and electromagnetic field, are, respectively,

$$R_{\alpha\beta} - \frac{1}{2}g_{\alpha\beta}R = 2(T^{\Psi}_{\alpha\beta} + T^{EM}_{\alpha\beta}) , \qquad \Box\Psi = \mu^2\Psi , \qquad D_\alpha F^{\alpha}{}_{\beta} = 0 , \tag{6.2}$$

where the two components of the energy-momentum tensor are

$$T^{\Psi}_{\alpha\beta} \equiv 2\partial_{(\alpha}\Psi^{*}\partial_{\beta)}\Psi - g_{\alpha\beta}\left(\partial_{\gamma}\Psi^{*}\partial^{\gamma}\Psi + \mu^{2}\Psi^{*}\Psi\right) , \tag{6.3}$$

$$T^{EM}_{\alpha\beta} \equiv F_{\alpha}{}^{\gamma}F_{\beta\gamma} - \frac{1}{4}g_{\alpha\beta}F_{\gamma\delta}F^{\gamma\delta} . \tag{6.4}$$

This model is invariant under a *global* transformation $\Psi \to \Psi e^{i\lambda}$, where λ is constant.

KNBHsUSH are obtained using the same metric and scalar field used to obtain the KBHsSH, Equation 5.14 and Equation 5.9, respectively, but now we also have an electromagnetic potential ansatz, which is given by,

$$A_{\alpha}dx^{\alpha} = (A_t - A_{\varphi}W\sin\theta)\,dt + A_{\varphi}\sin\theta d\varphi . \tag{6.5}$$

As for the functions in the metric and scalar field ansatz, A_t and A_{φ} also only depend on the spheroidal coordinates r and θ. Similar to the uncharged case we shall focus on the case $m = 1$ as an illustrative set of solutions, and also nodeless solution for the scalar field profile ϕ. Solutions with nodes will also exist, corresponding to excited states with higher ADM mass.

Now that we have the ansatz for the electromagnetic potential, in order to find KNBHsUSH, we have to impose boundary condition to it, in a identical way that we did for the metric function, in Section 3.1, and for the scalar field, in Subsection 5.2.2. In this way, we have the following boundary conditions:

(i) *Asymptotic boundary conditions.* Asymptotically flatness implies that the solution must approach a Minkowski spacetime at spatial infinity with vanishing matter field, thus,

$$\lim_{r\to\infty} A_{\varphi} = \lim_{r\to\infty} A_t = 0 . \tag{6.6}$$

Observe that the last equality could be changed to a constant, rather than zero, in a different gauge.

(ii) *Axis boundary conditions.* At the poles, *i.e.* at $\theta = 0, \pi$, axial symmetry and regularity imply,

$$\partial_{\theta}A_t = A_{\varphi} = 0 . \tag{6.7}$$

Also, due to the symmetry under reflections along the equatorial plane we can further impose the following boundary condition on the equatorial plane,

$$\partial_{\theta}A_t|_{\theta=\pi/2} = \partial_{\theta}A_{\varphi}|_{\theta=\pi/2} = 0 . \tag{6.8}$$

(iii) *Event horizon boundary conditions.* As done before several times, we can make a coordinate transformation in the form, $x = \sqrt{r^2 - r_H^2}$ to simplify the numerical treatment, and with this new coordinate one can compute a power series expansion near the horizon, $x \to 0$, of the electromagnetic potential,

$$A_t = \Phi_H + \mathcal{O}(x^2) , \tag{6.9}$$

$$A_{\phi} = A_{\varphi}^{(0)}(\theta) + \mathcal{O}(x^2) . \tag{6.10}$$

With this result it is natural to impose the following boundary condition,

$$A_t|_{r=r_H} = \Phi_H , \qquad \partial_x A_{\varphi}|_{r=r_H} = 0 . \tag{6.11}$$

For completness, let us state that the boundary conditions for the metric functions and the scalar field are similar to those described in the previous sections for configurations without a gauge field.

We also note that, since the scalar field is ungauged, it is identical to the scalar field in the KBHsSH case. Thus, despite of the electric charge of the BH in this case, the synchronization condition still stays the same as before,

$$\omega = m\Omega_H \ . \tag{6.12}$$

6.1.2 Physical Quantities

The KNBHsUSH are the electromagnetic generalization of KBHsSH, in the same way the KN BH is the electromagnetic generalization of Kerr BHs. As such, the physical quantities of these BHs are the same as those of KBHsSH but with a few new quantities. These new quantities are related to the electromagnetic field, now present around the BH, and consequently with the electromagnetic potential, A_α. Since the electromagnetic field carries energy and angular momentum, now the total mass and total angular momentum of the BH also have a term associated to the electromagnetic field,

$$M = M_H + M^\Psi + M^{EM} \ , \qquad J = J_H + J^\Psi + J^{EM} \ , \tag{6.13}$$

where, as before, M_H and J_H are the horizon mass and angular momentum, M^Ψ is the scalar field energy, which can be computed the same way as in Equation 5.23 and J^Ψ is the scalar field angular momentum, that is related with the same Noether charge as before, Equation 5.24, in a similar way, $J^\Psi = mQ$. The new terms, M^{EM} and J^{EM}, are the energy and angular momentum stored by the electromagnetic field outside the horizon.

The new solution will now possess an electric charge, Q_E, that can be computed using Gauss' law on any closed 2-surface covering the horizon. Alternatively, Q_E can be computed from the asymptotic behaviour of the electromagnetic potential, A_α, together with the magnetic dipole moment μ_M,

$$A_t = \frac{Q_E}{r} + \dots \ , \qquad A_\varphi = \frac{\mu_M \sin\theta}{r} + \dots \ . \tag{6.14}$$

As with the KN BHs, the gyromagnetic ratio g defines how the magnetic dipole moment is induced by the total angular momentum and charge, for a given mass,

$$\mu_M = g\frac{Q}{2M}J \ . \tag{6.15}$$

As a BH solution, KNBHsUSH must have a Smarr formula that related various quantities of interest. One can prove that such formula exists and can be written as,

$$M = 2T_H S + 2\Omega_H(J - mQ) + \Phi_H Q_E + M^\Psi \ , \tag{6.16}$$

where T_H and S are, respectively, the Hawking temperature and entropy, $S = A_H/4$, of the BH, and can be computed the same way as in Equation 3.18, and Φ_H is the electrostatic potential on the horizon. Such formula can yield a more generic 1st law of BH thermodynamics in comparison to the one for KBHsSH, Equation 5.27, which reads,

$$dM = T_H dS + \Omega_H dJ + \Phi_H dQ_E \ . \tag{6.17}$$

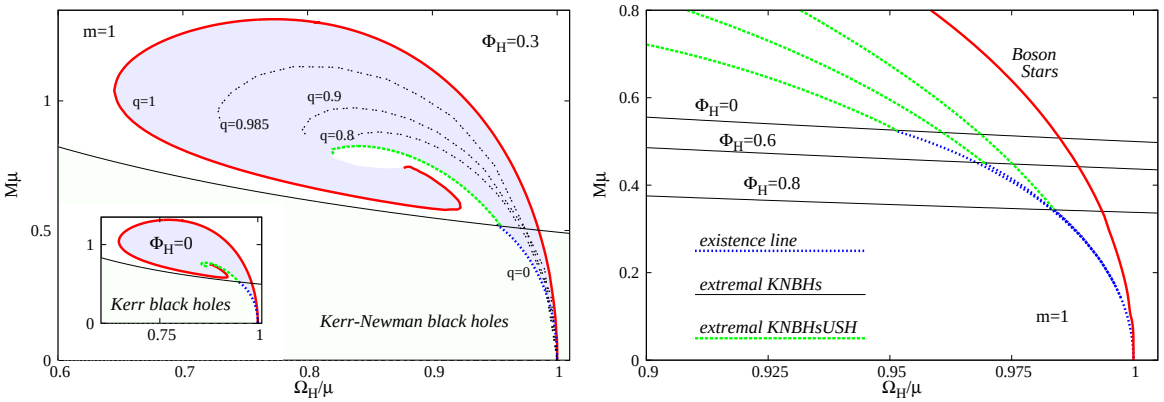

(a) (b)

Figure 6.1: The (Ω_H, M) domain of existence for a sample of a KNBHsUSH. (a) Diagram for $\Phi_H = 0.3$ with the boson star envelope (red solid line), the existence line on the domain of KN BHs (blue dotted line) and the line of extremal KNBHsUSH (green dashed line). The black solid line corresponds to the extremal KN BHs; non-extremal solutions exist below. The black dotted line have constant normalized Noether charge q. (Inset) diagram for $\Phi_H = 0$, corresponding to the KBHsSH case, for comparison. (b) Detail around the intersection of the existence lines with the extremal KNBHsUSH lines and the extremal KN lines for $\Phi_H = 0, 0.6$ and 0.8. Adapted from [16].

One can get a different Smarr relation, solely described by horizon quantities, by adding together Equation 5.22 and Equation 6.16,

$$M_H = 2T_H S + 2\Omega_H J_H \ , \tag{6.18}$$

where we also used the electromagnetic relation, $M^{EM} - 2\Omega_H J^{EM} - \Phi_H Q_E = 0$.

6.1.3 The Results

In order to find KNBHsUSH, the numerical integration is performed with dimensionless variables, in a similar way as in the previous chapter. In this way, all quantities of interest will be expressed in units set by μ. In particular this means we set $\mu Q_E \to Q_E$. Note that Φ_H is dimensionless in this type of units ($4\pi\epsilon_0 = 1$).

Let us start by giving an overview of the domain of existence of KNBHsUSH. For that we need to fix the new degree of freedom, which is related to the electric charge. An important observation here is that, similarly to the KN case, no solitonic limit exists, for a nonzero Q_E. Thus, for most of the numerical solutions we have chosen to fix the electrostatic potential on the horizon, Φ_H, and vary the remaining input parameters, Ω_H and r_H. This allows us to reach the solitonic limit, wherein the horizon area vanishes and the electrostatic potential becomes constant everywhere and pure gauge, and let us get a two-dimensional section of the full domain of existence as in the KBHsSH case – Figure 5.2a.

In Figure 6.1a, we present the (Ω_H, M) domain of existence of the solutions, where we fixed the electrostatic potential to be $\Phi_H = 0.3$. We point out that the domain presented was obtained by extrapolating into the continuum the results of a very large set of discrete solutions. We also remark that a qualitatively similar picture has been found for $\Phi_H = 0.6$.

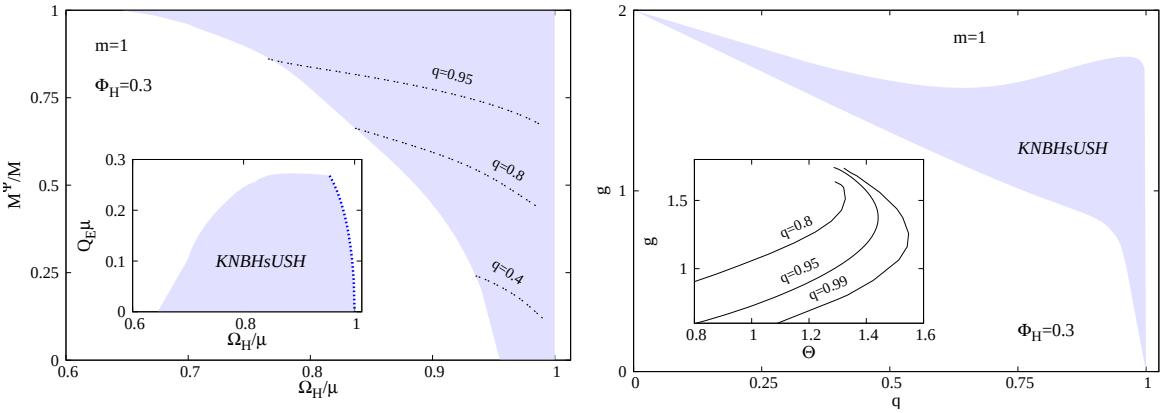

(a) (b)

Figure 6.2: (a) The ratio M^{Ψ}/M is shown as a function of Ω_H for a sample of KNBHsUSH. (Inset) The electric charge as a function of Ω_H, where the blue dotted line is the existence line. (b) The (q, g) diagram. (Inset) The gyromagnetic ratio as a function of Θ, which determines the KN bound, $\Theta \geq 1$. Adapted from [16].

As shown in the main panel (the inset is for $\Phi_H = 0$ – KBHsSH case, Figure 5.2a), this domain of existence is bounded by boson stars (red solid line), the KN limit (blue dotted line – dubbed *existence line*) and the extremal KNBHsUSH limit (green dashed line). As one can see in Figure 6.1b, if we increase the electrostatic potential, the lowest the mass of the extremal KN BH will be, along the existence line (henceforth dubbed as *Hod point*, following [54]) whence the line of extremal KNBHsUSH starts. These are expected results from the known behaviour of KN BHs. By closely examining the main panel with the inset in Figure 6.1a we can see that for higher Φ_H, there are extremal hairy BHs with lower horizon angular velocity.

In Figure 6.2a, we exhibit the ratio M^{Ψ}/M, which gives another measure of hairiness, as function of Ω_H for $\Phi_H = 0.3$. The figure shows that small fractions of the total energy in the hair are only allowed for sufficiently large horizon angular velocities. When the angular velocity is small, equilibrium between the hair and the horizon is only achievable with M^{Ψ}/M close to unity, which means that the normalized Noether charge q is close to unity, *i.e.*, boson star-like. The inset in this figure illustrates the (Ω_H, Q_E) domain of existence of the KNBHsUSH solutions. It shows that the electric charge of the solutions, for fixed Ω_H between that of the Hod point and the maximum allowed angular velocity, $\Omega_H = \mu$, is maximized along the existence line (and in particular at the Hod point). But for lower values of the angular velocity, the values of Q_E are maximized along the extremal KNBHsUSH line, and for some of these lower values of angular velocity, the electric charge is slightly bigger than that found at the Hod point.

Gyromagnetic Ratio

It is well known in Physics that rotating charges give rise to a magnetic dipole moment, μ_M. Such physical quantity is related with the total mass, angular momentum and electric charge as Equation 6.15 shows. In classical electromagnetism, for systems with constant ratio of charge to mass density, it was proven that the gyromagnetic ratio is $g = 1$. But

in the beginning of the 20th century, Stern and Gerlach performed their famous experiment where they show that the gyromagnetic ratio of the electron should be $g = 2$ instead of the expected $g = 1$. With this discovery it became clear that a new fundamental description for the electron was necessary, beyond the scope of the non-relativistic quantum theory. Such a description appeared with Dirac equation, which predicts $g = 2$, a value that is corrected by loop diagrams in Quantum Electrodynamics (QED), yielding the so called anomalous magnetic moment, whose agreement with the experiments is one of the outstanding successes of QED.

In BH physics, Carter was the first to report the gyromagnetic ratio of a KN BH [15], showing that the gyromagnetic ratio of a KN BH is the same as the electron's, $g = 2$. Since then many other studies considered the gyromagnetic ratio of rotating charged BHs, for instance, with different asymptotics and in higher dimensions (see *e.g.* [55, 56, 57]). Here we show that the addition of scalar hair leads to a suppression of the gyromagnetic ratio, and of the corresponding magnetic dipole moment, with respect to that a comparable KN BH. A novel aspect is that g can be smaller than 1, a rather unusual feature in other models of relativistic, charged and spinning compact objects, *cf.* [58].

In Figure 6.2b, we present the gyromagnetic ratio in a (q, g) diagram for KNBHsUSH with $\Phi_H = 0.3$. In this diagram we can see that the gyromagnetic ratio, g, of both the extremal and non-extremal hairy BH solutions, is always less than 2, and as expected, it is only equal to 2 in the limit of vanishing hair. To have a better insight we introduced the quantity,

$$\Theta \equiv \frac{M^2}{Q_E^2 + J^2/M^2} \ , \tag{6.19}$$

which determines the KN bound, $\Theta \geq 1$, which holds for all KN BHs. However, this bound is strongly violated by a large set of KNBHsUSH, in particular by those close to the BS limit, as easily seen in Figure 6.1a. This is very reminiscent of what happen for KBHsSH, as we saw in Figure 5.2a. In the inset of Figure 6.2b, one can see the gyromagnetic ratio as function of Θ and conclude that solutions with $g < 1$ predominantly exhibit $\Theta < 1$ and thus violating the KN bound.

6.2 Gauged Scalar Field Model

6.2.1 Main Differences in the Model

We will now consider the model described in Section 6.1 but with a *gauged* scalar field, that couples minimally to the electromagnetic field, with gauge coupling q_G. This coupling is implemented by replacing the partial derivatives of the scalar field in the action, Equation 6.1, as

$$\partial_\alpha \Psi \longrightarrow D_\alpha \Psi = \partial_\alpha \Psi + i q_G A_\alpha \Psi \ . \tag{6.20}$$

The Einstein equations still take the form in Equation 6.1 but with the above substitution in the scalar field energy-momentum tensor, Equation 6.3. The scalar and Maxwell equations of motion now become

$$D_\alpha D^\alpha \Psi = \mu^2 \Psi \ , \qquad \nabla_\beta F^{\beta\alpha} = i q_G \left[\left(D^\alpha \Psi^* \right) \Psi - \Psi^* \left(D^\alpha \Psi \right) \right] \equiv q_G j^\alpha \ . \tag{6.21}$$

Physically this means that the scalar field is now electrically charged (each scalar particle carries a charge q_G), and thus the scalar field sources the Maxwell field.

Unlike for the previous model, where it was invariant under a *global* transformation, $\Psi \to \Psi e^{i\lambda}$, this new model is invariant under a *local* $U(1)$ gauge transformation,

$$\Psi \to \Psi e^{iq_G\lambda} , \qquad A_\alpha \to A_\alpha + \partial_\alpha \lambda , \tag{6.22}$$

where λ is now a real function of the spacetime coordinates. One consequence of this gauge invariance is that the (t, φ)-dependence of the scalar field ansatz, Equation 5.9, can now be gauged away by applying the *local* $U(1)$ symmetry, Equation 6.22, with $\lambda = (m\varphi - \omega t)/q_G$. However, this also changes the gauge field as $A_t \to A_t - \omega/q_G$ and $A_\varphi \to A_\varphi + m/q_G$. Consequently, the solutions cannot be constructed starting with the configurations in the previous section and increasing q_G. Thus, in order to be able to consider this approach, we keep the (t, φ)-dependence in the scalar field ansatz and fix the corresponding gauge freedom by setting $A_t = A_\varphi = 0$ at infinity.

One major difference with respect to the ungauged case is that the solitonic limit of the solutions carries now a nonzero electric charge. The Noether charge Q of the solitons, *i.e.* the total particle number, is now intrinsically related to the electric charge Q_E. The former can be computed as [1],

$$Q = \int d^3x\sqrt{-g}j^t = 4\pi \int_{r_H}^{\infty} dr \int_0^{\pi} d\theta r^2 \sin\theta e^{-F_0+2F_1+F_2} \left(\omega - q_G A_t - mW\right) \phi^2 , \tag{6.23}$$

whereas the latter can be read from the asymptotics of the electric potential, Equation 6.14, or can be calculated through Equation 4.7, where $Q_E^{(H)} = 0$ since we are in the solitonic limit. A straightforward computation shows that both the Noether charge and the electric charge of the spinning solitons are proportional to the total angular momentum,

$$J = mQ = 4\pi \frac{mQ_E}{q_G} . \tag{6.24}$$

6.2.2 Features of the Gauge Scalar Field Solutions

The construction of the gauged scalar field solutions is similar to that described above for the ungauged case, $q_G = 0$. In particular, KNBHsGSH are subject to the same set of boundary conditions used in the ungauged case. However, the synchronization condition is now,

$$\omega - q_G\Phi_H = m\Omega_H , \tag{6.25}$$

in agreement with the results from the linear theory [47, 48].

The electrically charged boson stars are an important part of the domain of existence of KNBHsGSH, as for the ungauged case, and for that reason we will pay special attention to this limiting case. These solutions are obtained by considering the same ansatz as before, Equation 5.14, Equation 5.9 and Equation 6.5, but with $r_H = 0$ and replacing the horizon's boundary conditions, mentioned in Subsection 6.1.1, by the following boundary conditions at the origin

$$\partial_r F_i|_{r=0} = W|_{r=0} = 0 , \quad \phi|_{r=0} = 0 , \quad \partial_r A_t|_{r=0} = A_\varphi|_{r=0} = 0 . \tag{6.26}$$

In Figure 6.3a we can see some results of the numerical integration. The basic properties of the spinning gauged boson stars solutions can be summarized as follows. First, for all values

[1] We recall that for solitons $r_H = 0$, therefore $N = 1$ in the general metric ansatz.

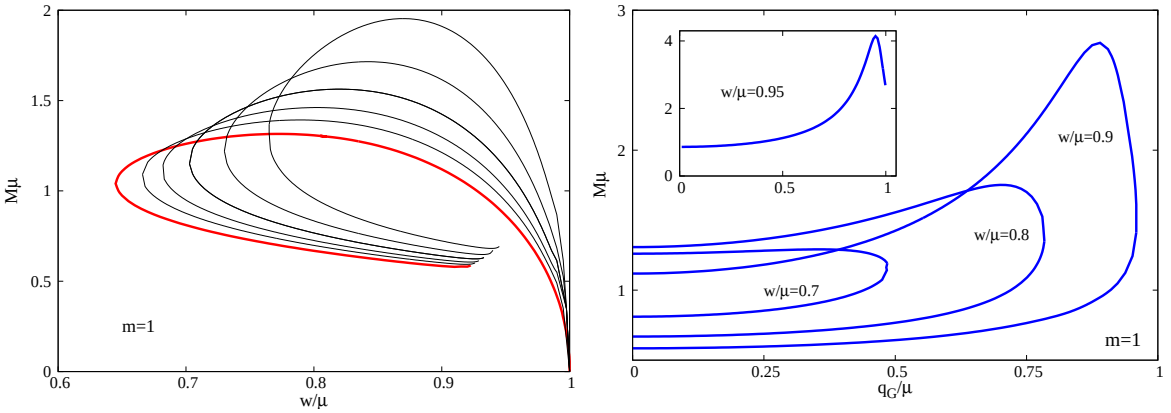

(a) (b)

Figure 6.3: (a) The (ω, M) diagram for spinning BS with $q_G = 0$ (red curve), $q_G/\mu = 0.2, 0.3, 0.4, 0.5$ and 0.6 (top curve). (b) The mas M is shown as a function of the gauge coupling constant q_G for several frequencies, $\omega/\mu = 0.7, 0.8, 0.9$ and 0.95 (as an inset). Adapted from [16].

---

of the gauge coupling considered, the frequency dependence of the solutions is qualitatively similar to the ungauged case. The solutions exist for a limited range of frequencies $[\omega_{min}, \mu]$. In particular, we observe that the minimal frequency, ω_{min}, increases with q_G. After this minimal frequency, a backbending towards larger values of ω occurs, yielding a second branch of solutions. Following this second branch of solutions, we arrive to a maximum value of the frequency, ω_{max}, which increases again with q_G, but never exceeds μ. Then, similarly to the ungauged case, a third branch of solutions develops – not shown in Figure 6.3a. Subsequently, we expect the existence of an inspiraling behaviour of the solutions, in analogy with uncharged boson stars, towards a limiting configuration. Second, the maximal mass of spinning gauged boson stars increases with q_G.

A similar behaviour was found to the (ω, J) diagram, where the total angular momentum also spiral towards a limiting configuration. Consequently, the axially symmetric gauged boson stars do not possess a static limit.

As shown in Figure 6.3b, the solutions possess also a nontrivial dependence on the gauge coupling constant q_G. For given values of ω, spinning solutions only exist up to a maximal value of the gauge coupling constant, $q_G = (q_G)_{max}$. For $(q_G)_{max}$ the charge repulsion becomes bigger than the scalar and gravitational attraction and localized solutions cease to exist (we point out to the fact that the maximal value of q_G increases with the frequency). This behaviour is quite similar to that discussed for the spherically symmetric case [59, 60]. Also, as seen in Figure 6.3b, all global charges stay finite as $q_G \to (q_G)_{max}$.

Now that we know how the spinning gauged solitons behave, we can discuss KNBHsGSH. They are obtained by adding a horizon at the center of the above solutions. One way to construct the BHs is to start from the boson stars and slightly increase the horizon size via the parameter r_H and fixing the other input parameters, Ω_H, q_G, Φ_H and m. We recall that for this BHs the frequency ω is fixed by the synchronization condition, Equation 6.25. Then one finds three possible behaviours for the resulting branches of BH solutions, as seen in Figure 6.4. First (i), for small enough values of Ω_H, the branch of BHs connects two differents boson stars; as $r_H \to 0$ the horizon area vanishes, $q \to 1$, while the temperature diverges. For

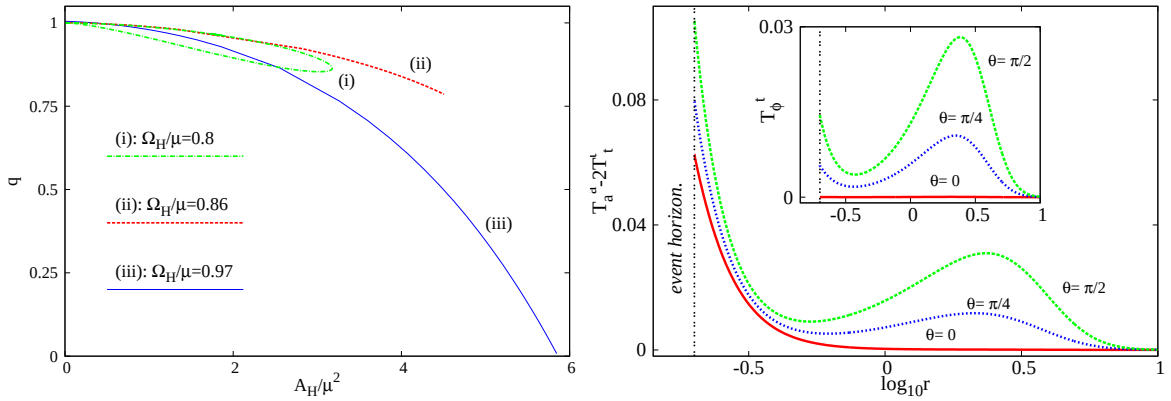

(a) (b)

Figure 6.4: (a) The (A_H, q) diagram is shown for three sets of KNBHsGSH solutions with fixed values of Ω/μ and $q_G/\mu = 0.2$, $\Phi_H = 0.1$. (b) Energy density (and angular momentum density in the inset) along three different slices of constant θ for an illustrative example of a KNBHGSH. Adapted from [16].

---

intermediate values of Ω_H, the branch of solutions ends in an extremal KNBHsGSH solution (ii); these limiting configurations have finite horizon size and global charges, $0 < q < 1$ and appear to possess a regular horizon. Finally (iii), for large enough of Ω_H, the branch of KNBHsGSH interpolates between a charged boson star and a set of critical KN solutions, which have $q = 0$ and $A_H > 0$, and lies again on the *existence line*.

In Figure 6.4b we exhibit the Komar energy density and angular momentum density (in the inset) for an illustrative example of a KNBHGSH with physical input parameters $r_H = 0.24$, $\omega = 0.86$, $q_G = 0.2$ and $\Phi_H = 0.1$. These densities have a contribution from both the electromagnetic and the scalar field. The main feature we wish to emphasize is the composite structure revealed by the plots. KN BHs have an electromagnetic energy and angular momentum density that decay with the radial coordinate, whereas boson stars have a toroidal-like distributions for the scalar energy and angular momentum density. Consequently, KNBHsGSH exhibit a superposition of these two behaviours, with decaying densities from the horizon but which exhibit a local maximum, in the neighbourhood of the equatorial plane, at some finite radial coordinate. Although not shown in this thesis, a similar energy and angular momentum distribution was found to the KNBHsUSH case.

The behaviours illustrated in Figure 6.4 support the expectation that the domain of existence of KNBHsGSH will be fill in a similar fashion as the KNBHsUSH case, Figure 6.1a, delimited by the solitonic limit curves exhibited in Figure 6.1a, together with the existence line of KN BHs and a line of extremal KNBHsGSH. One last behaviour that also supports this expectation is the fact that the gyromagnetic ratio is always smaller than $g = 2$, as we show in the KNBHsUSH case.

Chapter 7

Conclusion

Throughout this thesis, two main topics were discussed: the physical quantities of a BH and hairy BHs.

In the former topic, we have pointed out that well known, in closed form, asymptotically flat, charged rotating BH solutions violate the Kerr bound in terms of horizon quantities. Furthermore, the KN BH family even violates the RN bound in terms of horizon quantities, in particular in the static limit, where we have the RN solution. This surprising result, to best of our knowledge, had not been explicitly shown in the literature, and it shows that the Kerr bound and RN bound may not be so fundamental as one originally thought, specially in terms of horizon quantities. We have also shown that such violations are independent of the presence of "matter" outside the horizon, since we observed violations in both the "bald" BHs – Kerr-Newman – and in BHs that have a secondary (non-independent scalar) hair – Kerr-Sen. These violations may be explained by the fact that there is energy outside the BHs (due to the fields) and that implies the existence of matter outside the horizon, by the relativistic energy equivalent, and since the BHs are rotating, they have to "drag" this matter, increasing the momentum of inertia, and thus more dimensionless angular momentum is permitted within the horizon, without increasing the angular velocity to values incompatible with the existence of a horizon [30, 61].

In the latter topic, we have shown that regular, axisymmetric, stationary and asymptotically flat BHs can have scalar hair, despite the multiple theorems that show otherwise, in particular the famous Bekenstein's theorem. Such BHs were dubbed Kerr BHs with scalar hair. They exist at the threshold of the superrandiance regime and have some special properties compared to "bald" BHs. Two of these properties are the quadrupole moment and the shadows. Both properties have a big astrophysical interest, since both of them can be measured. For the former, KBHsSH can have a quadrupole moment one to two order of magnitude larger than a Kerr BH with the same mass and angular momentum [6]. As for the latter, the shadow of a KBHsSH have a strong dependence with the scalar hair, meaning that a Kerr BH (no scalar hair) with some mass and angular momentum will have a different shadow as a KBHsSH with the same mass and angular momentum [62].

Still in the hairy BH topic, we gave an electric generalization of the KBHsSH – the Kerr-Newman BHs with scalar hair (KNBHsSH). Such BHs were divided in two sets of BHs, one with ungauged scalar hair, and another with gauged scalar hair. For both cases we saw a similar behaviour as the KBHsSH, in the same way the Kerr-Newman solution has a similar behaviour as the Kerr one. The most interesting new physical property discussed here was

the fact that, for both the ungauged and gauged case, the gyromagnetic ratio is always $g \leq 2$, with equality attained only in the "bald" case. This result implies that the scalar hair leads to a suppression of the magnetic dipole moment, and such suppression may be seen if one computes the electromagnetic field lines. For this type of BH, there is much work one can still do to obtain a better understanding of these BHs. We can perform similar studies as one did for the KBHsSH case, namely compute the quadrupole moment and their shadows to see the signatures that these BHs have and if it is possible to distinguish them from other type of BHs. Another task one can do, that we have already mentioned above for these electrically charged BHs, is to compute their electric and magnetic fields lines, and try to understand better the reason behind the inequality for the gyromagnetic ratio, $g \leqslant 2$.

Appendix A

New Coordinates for Kerr black hole

Throughout this thesis we have used a generic axially symmetric metric ansatz for the numerical integration of our solutions. Such metric reads

$$ds^2 = -e^{2F_0} N dt^2 + e^{2F_1}\left(\frac{dr^2}{N} + r^2 d\theta^2\right) + e^{2F_2} r^2 \sin^2\theta (d\varphi - W dt)^2 \,, \tag{A.1}$$

with $N \equiv 1 - r_H/r$ and F_0, F_1, F_2, W functions of r, θ.

In the vacuum case, as stated in Section 3.1, this is exactly the Kerr metric but written in a non-standard coordinate system. The metric functions can be written as [7],

$$e^{2F_1} = \left(1 - \frac{c_t}{r}\right)^2 + c_t\,(c_t - r_H)\,\frac{\cos^2\theta}{r^2} \,, \tag{A.2}$$

$$e^{2F_2} = e^{-2F_1}\left\{\left[\left(1 - \frac{c_t}{r}\right)^2 + \frac{c_t\,(c_t - r_H)}{r^2}\right]^2 + c_t\,(r_H - c_t)\left(1 - \frac{r_H}{r}\right)\frac{\sin^2\theta}{r^2}\right\} \,, \tag{A.3}$$

$$F_0 = -F_2 \,, \qquad W = \frac{e^{-2(F_1+F_2)}}{r^3}\sqrt{c_t\,(c_t - r_H)}\,(r_H - 2c_t)\left(1 - \frac{c_t}{r}\right) \,, \tag{A.4}$$

where r_H, as before, is the horizon radius and $c_t < 0$ is a constant that, as it is, does not have a very transparent meaning; however, it can taken as a measure of non-staticity, since $c_t = 0$ is the Schwarzschild metric.

With such metric and expression for the metric functions, one can computed the various physical quantities of interest [7],

$$M = \frac{1}{2}(r_H - 2c_t) \,, \qquad J = \frac{1}{2}\sqrt{c_t\,(c_t - r_H)}\,(r_H - 2c_t) \,, \tag{A.5}$$

$$A_H = 4\pi\,(r_H - c_t)\,(r_H - 2c_t) \,, \qquad T_H = \frac{r_H}{4\pi\,(r_H - c_t)\,(r_H - 2c_t)} \,, \tag{A.6}$$

$$\Omega_H = \frac{\sqrt{c_t\,(c_t - r_H)}}{(r_H - c_t)\,(r_H - 2c_t)} \,. \tag{A.7}$$

We note that the formal limit $r_H = 2c_t$ corresponds to the flat space in an unusual coordinate system.

The relation between the radial coordinate above, r, and the radial coordinate of the Kerr metric in BL coordinates, R, is [7],

$$r = R - \frac{a^2}{R_H} \,, \tag{A.8}$$

where $R_H = M + \sqrt{M^2 - a^2}$ is the horizon radius of the Kerr metric in BL coordinates, and $a = J/M$. With this relation, we can obtain an expression that connects the horizon radius in the unusual coordinates with the BL's horizon radius,

$$r_H = R_H - \frac{a^2}{R_H} \,. \tag{A.9}$$

Through this new equation we can see that for an extremal Kerr BH, $r_H \to 0$. The other coordinates, t, θ and φ, are the same for both parametrizations.

If one takes a closer look to the physical quantities computed above, one can see that, with the following transformation,

$$c_t = r_H u \,, \tag{A.10}$$

those equations simplify, making transparent the connection with the Schwarzschild limit,

$$M = \frac{r_H}{2}\left(1 - 2u\right) \,, \qquad J = \frac{r_H^2}{2}\sqrt{u\left(u-1\right)}\left(1-2u\right) \,, \tag{A.11}$$

$$A_H = 4\pi r_H^2 \left(1-u\right)\left(1-2u\right) \,, \qquad T_H = \frac{1}{4\pi r_H^2}\frac{1}{\left(1-u\right)\left(1-2u\right)} \,, \tag{A.12}$$

$$\Omega_H = \frac{1}{r_H}\frac{\sqrt{u\left(u-1\right)}}{\left(1-u\right)\left(1-2u\right)} \,, \tag{A.13}$$

which happens when we take $u \to 0$.

In practice, the input parameters in our solver are r_H and Ω_H, then one uses Equation A.13 to express u as a function of $x = \Omega_H r_H$. This reveals the existence of two branches of solutions. The first branch has

$$u = u^{(low)} = \frac{1}{3}\left\{2 + \frac{\sqrt{3+x^2}}{x}\cos\left[\frac{1}{3}\left(4\pi + \arccos\left[\frac{x\left(18+x^2\right)}{\left(3+x^2\right)^{3/2}}\right]\right)\right]\right\} \,, \tag{A.14}$$

and starts from a static Schwarzschild configuration, since when $x \to 0$, $u \to 0$, thus, all physical quantities become the Schwarzschild one. The second branch has,

$$u = u^{(up)} = \frac{1}{3}\left\{2 + \frac{\sqrt{3+x^2}}{x}\cos\left[\frac{1}{3}\left(2\pi + \arccos\left[\frac{x\left(18+x^2\right)}{\left(3+x^2\right)^{3/2}}\right]\right)\right]\right\} \,, \tag{A.15}$$

but, different from the 1st branch, this branch approaches an extremal Kerr solution as $x \to 0$, since $u \to \infty$. These two branches meet for a maximal values of x, $x^{(max)} = \sqrt{\left(5\sqrt{5}-11\right)/2} = 0.300283106..$.

In Figure A.1 and Figure A.2, we can see clearly the existence of two branches and that they meet around $x \simeq 0.3$, for the four physical quantities.

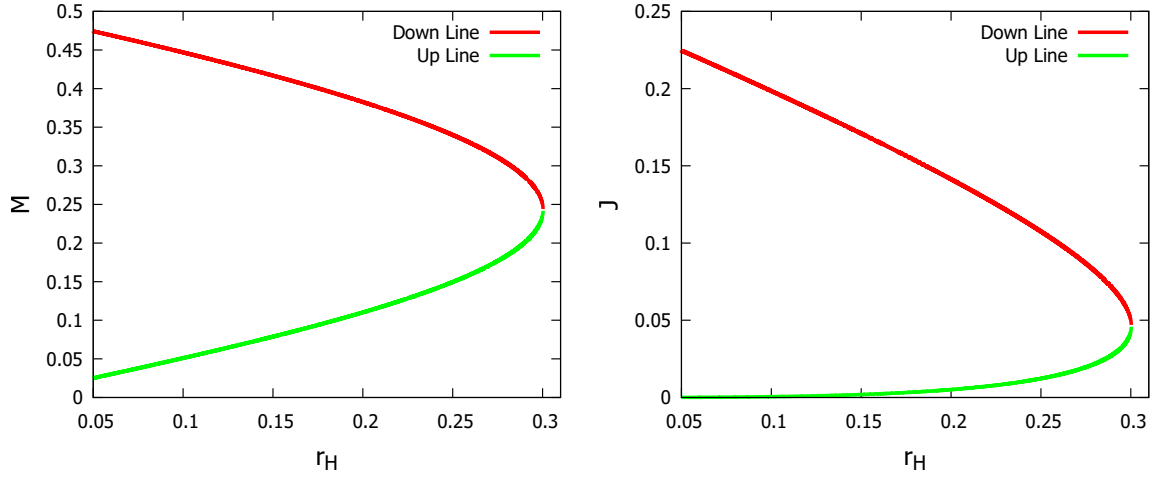

(a) (b)

Figure A.1: The mass (a) and angular momentum (b) are shown as a function of the horizon radius, r_H, for a fixed value of the horizon angular velocity, $\Omega_H = 1$. One can observe the existence of two branches of solutions.

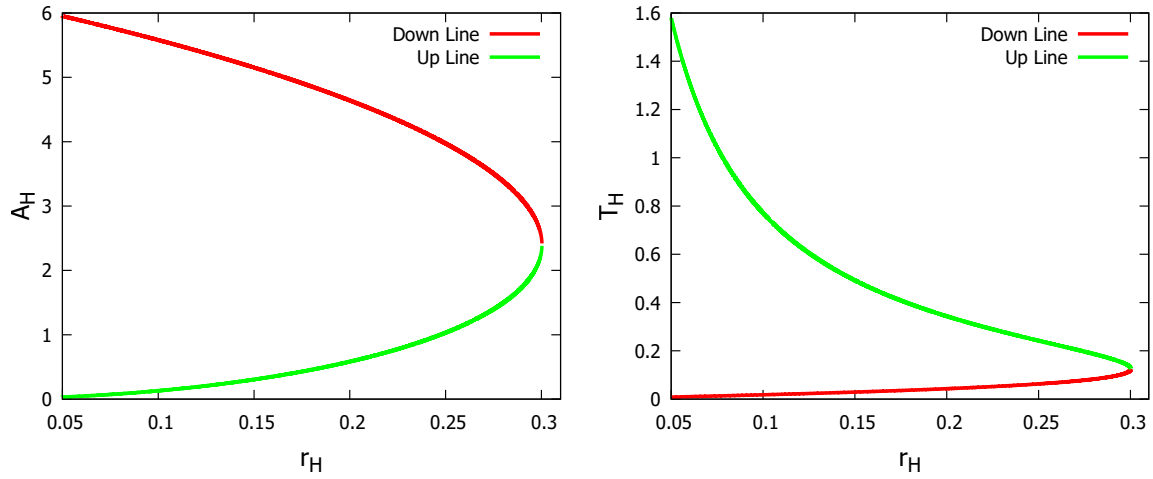

(a) (b)

Figure A.2: The horizon area (a) and Hawking temperature (b) are shown as a function of the horizon radius, r_H, for a fixed value of the horizon angular velocity, $\Omega_H = 1$. One can observe, again, the existence of two branches of solutions.

Bibliography

[1] B. P. Abbott *et al.*, "Observation of Gravitational Waves from a Binary Black Hole Merger," *Phys. Rev. Lett.*, vol. 116, no. 6, p. 061102, 2016.

[2] E. Berti *et al.*, "Testing General Relativity with Present and Future Astrophysical Observations," *Class. Quant. Grav.*, vol. 32, p. 243001, 2015.

[3] P. T. Chrusciel, J. Lopes Costa, and M. Heusler, "Stationary Black Holes: Uniqueness and Beyond," *Living Rev. Rel.*, vol. 15, p. 7, 2012.

[4] R. P. Kerr, "Gravitational field of a spinning mass as an example of algebraically special metrics," *Phys. Rev. Lett.*, vol. 11, pp. 237–238, 1963.

[5] R. Ruffini and J. A. Wheeler, "Introducing the black hole," *Phys. Today*, vol. 24, no. 1, p. 30, 1971.

[6] C. A. R. Herdeiro and E. Radu, "Kerr black holes with scalar hair," *Phys. Rev. Lett.*, vol. 112, p. 221101, 2014.

[7] C. Herdeiro and E. Radu, "Construction and physical properties of Kerr black holes with scalar hair," *Class. Quant. Grav.*, vol. 32, no. 14, p. 144001, 2015.

[8] F. E. Schunck and E. W. Mielke, "General relativistic boson stars," *Class. Quant. Grav.*, vol. 20, pp. R301–R356, 2003.

[9] C. A. R. Herdeiro and E. Radu, "A new spin on black hole hair," *Int. J. Mod. Phys.*, vol. D23, no. 12, p. 1442014, 2014.

[10] C. A. R. Herdeiro, E. Radu, and H. Rúnarsson, "Kerr black holes with self-interacting scalar hair: hairier but not heavier," *Phys. Rev.*, vol. D92, no. 8, p. 084059, 2015.

[11] C. Herdeiro, E. Radu, and H. Runarsson, "Kerr black holes with Proca hair," *Class. Quant. Grav.*, vol. 33, no. 15, p. 154001, 2016.

[12] E. T. Newman, R. Couch, K. Chinnapared, A. Exton, A. Prakash, and R. Torrence, "Metric of a Rotating, Charged Mass," *J. Math. Phys.*, vol. 6, pp. 918–919, 1965.

[13] A. Sen, "Rotating charged black hole solution in heterotic string theory," *Phys. Rev. Lett.*, vol. 69, pp. 1006–1009, 1992.

[14] J. F. M. Delgado, C. A. R. Herdeiro, and E. Radu, "Violations of the Kerr and Reissner-Nordström bounds: Horizon versus asymptotic quantities," *Phys. Rev.*, vol. D94, no. 2, p. 024006, 2016.

[15] B. Carter, "Global structure of the Kerr family of gravitational fields," *Phys. Rev.*, vol. 174, pp. 1559–1571, 1968.

[16] J. F. M. Delgado, C. A. R. Herdeiro, E. Radu, and H. Rúnarsson, "Kerr-Newman black holes with scalar hair," *Physics Letters B*, vol. 761, pp. 234 – 241, 2016.

[17] K. Schwarzschild, "On the gravitational field of a mass point according to Einstein's theory," *Sitzungsber. Preuss. Akad. Wiss. Berlin (Math. Phys.)*, vol. 1916, pp. 189–196, 1916.

[18] H. Reissner, "Über die eigengravitation des elektrischen feldes nach der einsteinschen theorie," *Annalen der Physik*, vol. 355, no. 9, pp. 106–120, 1916.

[19] G. Nordstrom, "On the energy of the gravitational field in einstein's theory," *Verhandl. Koninkl. Ned. Akad. Wetenschap., Afdel. Natuurk.*, vol. 26, p. 1201–1208, 1918.

[20] W. Schönauer and E. Schnepf, "Software considerations for the "black box"; solver fidisol for partial differential equations," *ACM Trans. Math. Softw.*, vol. 13, pp. 333–349, Dec. 1987.

[21] W. Schönauer and R. Weiβ, "Special issue on parallel algorithms for numerical linear algebra efficient vectorizable pde solvers," *Journal of Computational and Applied Mathematics*, vol. 27, no. 1, pp. 279 – 297, 1989.

[22] W. Schönauer and T. Adolph, "How we solve pdes," *Journal of Computational and Applied Mathematics*, vol. 131, no. 1–2, pp. 473 – 492, 2001.

[23] P. Grandclement, C. Somé, and E. Gourgoulhon, "Models of rotating boson stars and geodesics around them: new type of orbits," *Phys. Rev.*, vol. D90, no. 2, p. 024068, 2014.

[24] S. W. Hawking, "Particle creation by black holes," *Communications in Mathematical Physics*, vol. 43, no. 3, pp. 199–220, 1975.

[25] E. Poisson, *A Relativist's Toolkit: The Mathematics of Black-Hole Mechanics*. Cambridge University Press, 2004.

[26] A. Komar, "Positive-definite energy density and global consequences for general relativity," *Phys. Rev.*, vol. 129, pp. 1873–1876, Feb 1963.

[27] S. Q. Wu and X. Cai, "Massive complex scalar field in the kerr–sen geometry: Exact solution of wave equation and hawking radiation," *Journal of Mathematical Physics*, vol. 44, no. 3, pp. 1084–1088, 2003.

[28] G. W. Gibbons, C. A. R. Herdeiro, C. M. Warnick, and M. C. Werner, "Stationary Metrics and Optical Zermelo-Randers-Finsler Geometry," *Phys. Rev.*, vol. D79, p. 044022, 2009.

[29] L. Smarr, "Mass formula for kerr black holes," *Phys. Rev. Lett.*, vol. 30, pp. 71–73, Jan 1973.

[30] C. A. R. Herdeiro and E. Radu, "How fast can a black hole rotate?," *Int. J. Mod. Phys.*, vol. D24, no. 12, p. 1544022, 2015.

[31] D. Wiltshire, M. Visser, and S. Scott, *The Kerr Spacetime: Rotating Black Holes in General Relativity*. Cambridge University Press, 2009.

[32] G. Aad *et al.*, "Observation of a new particle in the search for the Standard Model Higgs boson with the ATLAS detector at the LHC," *Phys. Lett.*, vol. B716, pp. 1–29, 2012.

[33] S. Chatrchyan *et al.*, "Observation of a new boson at a mass of 125 GeV with the CMS experiment at the LHC," *Phys. Lett.*, vol. B716, pp. 30–61, 2012.

[34] V. Faraoni, "The correspondence between a scalar field and an effective perfect fluid," *Phys. Rev.*, vol. D85, p. 024040, 2012.

[35] C. A. R. Herdeiro and E. Radu, "Asymptotically flat black holes with scalar hair: a review," *Int. J. Mod. Phys.*, vol. D24, no. 09, p. 1542014, 2015.

[36] J. D. Bekenstein, "Nonexistence of baryon number for static black holes," *Phys. Rev. D*, vol. 5, pp. 1239–1246, Mar 1972.

[37] J. D. Bekenstein, "Nonexistence of baryon number for black holes. ii," *Phys. Rev. D*, vol. 5, pp. 2403–2412, May 1972.

[38] S. W. Hawking, "Black holes in general relativity," *Communications in Mathematical Physics*, vol. 25, no. 2, pp. 152–166, 1972.

[39] S. L. Liebling and C. Palenzuela, "Dynamical Boson Stars," *Living Rev. Rel.*, vol. 15, p. 6, 2012.

[40] D. J. Kaup, "Klein-gordon geon," *Phys. Rev.*, vol. 172, pp. 1331–1342, Aug 1968.

[41] R. Ruffini and S. Bonazzola, "Systems of self-gravitating particles in general relativity and the concept of an equation of state," *Phys. Rev.*, vol. 187, pp. 1767–1783, Nov 1969.

[42] S. A. Teukolsky, "Rotating black holes: Separable wave equations for gravitational and electromagnetic perturbations," *Phys. Rev. Lett.*, vol. 29, pp. 1114–1118, Oct 1972.

[43] J. Barranco, A. Bernal, J. C. Degollado, A. Diez-Tejedor, M. Megevand, M. Alcubierre, D. Núñez, and O. Sarbach, "Are black holes a serious threat to scalar field dark matter models?," *Phys. Rev. D*, vol. 84, p. 083008, Oct 2011.

[44] R. Brito, V. Cardoso, and P. Pani, "Superradiance," *Lect. Notes Phys.*, vol. 906, pp. pp.1–237, 2015.

[45] S. Hod, "Stationary Scalar Clouds Around Rotating Black Holes," *Phys. Rev.*, vol. D86, p. 104026, 2012. [Erratum: Phys. Rev.D86,129902(2012)].

[46] S. Hod, "Stationary resonances of rapidly-rotating Kerr black holes," *Eur. Phys. J.*, vol. C73, no. 4, p. 2378, 2013.

[47] S. Hod, "Kerr-Newman black holes with stationary charged scalar clouds," *Phys. Rev.*, vol. D90, no. 2, p. 024051, 2014.

[48] C. L. Benone, L. C. B. Crispino, C. Herdeiro, and E. Radu, "Kerr-Newman scalar clouds," *Phys. Rev.*, vol. D90, no. 10, p. 104024, 2014.

[49] F. E. Schunck and E. W. Mielke, "Rotating boson star as an effective mass torus in general relativity," *Physics Letters A*, vol. 249, no. 5, pp. 389 – 394, 1998.

[50] S. Yoshida and Y. Eriguchi, "Rotating boson stars in general relativity," *Phys. Rev. D*, vol. 56, pp. 762–771, Jul 1997.

[51] F. D. Ryan, "Spinning boson stars with large self-interaction," *Phys. Rev. D*, vol. 55, pp. 6081–6091, May 1997.

[52] I. Peña and D. Sudarsky, "Do collapsed boson stars result in new types of black holes?," *Classical and Quantum Gravity*, vol. 14, no. 11, p. 3131, 1997.

[53] V. Cardoso, C. F. B. Macedo, P. Pani, and V. Ferrari, "Black holes and gravitational waves in models of minicharged dark matter," *JCAP*, vol. 1605, no. 05, p. 054, 2016.

[54] C. A. R. Herdeiro, E. Radu, and H. Rúnarsson, "Kerr black holes with self-interacting scalar hair: Hairier but not heavier," *Phys. Rev. D*, vol. 92, p. 084059, Oct 2015.

[55] C. A. R. Herdeiro, "Special properties of five-dimensional BPS rotating black holes," *Nucl. Phys.*, vol. B582, pp. 363–392, 2000.

[56] D. Garfinkle and J. H. Traschen, "On the Gyromagnetic Ratio of a Black Hole," *Phys. Rev.*, vol. D42, pp. 419–423, 1990.

[57] A. N. Aliev, "Gyromagnetic Ratio of Charged Kerr-Anti-de Sitter Black Holes," *Class. Quant. Grav.*, vol. 24, pp. 4669–4678, 2007.

[58] J. Novak and E. Marcq, "Gyromagnetic ratio of rapidly rotating compact stars in general relativity," *Class. Quant. Grav.*, vol. 20, pp. 3051–3060, 2003.

[59] P. Jetzer and J. J. van der Bij, "Charged Boson Stars," *Phys. Lett.*, vol. B227, pp. 341–346, 1989.

[60] D. Pugliese, H. Quevedo, J. A. Rueda H., and R. Ruffini, "Charged boson stars," *Phys. Rev. D*, vol. 88, p. 024053, Jul 2013.

[61] C. A. R. Herdeiro, C. Rebelo, and C. M. Warnick, "On the backreaction of frame dragging," *Phys. Rev.*, vol. D80, p. 084037, 2009.

[62] P. V. P. Cunha, C. A. R. Herdeiro, E. Radu, and H. F. Runarsson, "Shadows of Kerr black holes with scalar hair," *Phys. Rev. Lett.*, vol. 115, no. 21, p. 211102, 2015.